MAINZER MIKROTRON

SFB 443

Hadron Physics at the Mainz Microtron MAMI

Thomas Walcher
Institut für Kernphysik
Johannes Gutenberg-Universität Mainz, Germany

1. **Introduction:** Why and how hadron physics?
2. **Recent highlights of MAMI**
   - Form factors of the nucleon
   - Pion polarizability
3. **MAMI C**
   - Energy increase to 1500 MeV: MAMI C
   - CB@MAMI
   - KAOS@MAMI
4. **Extended oportunities at MAMI C**
   - overview
   - nucleon resonances in selective decay channels
5. Conclusions

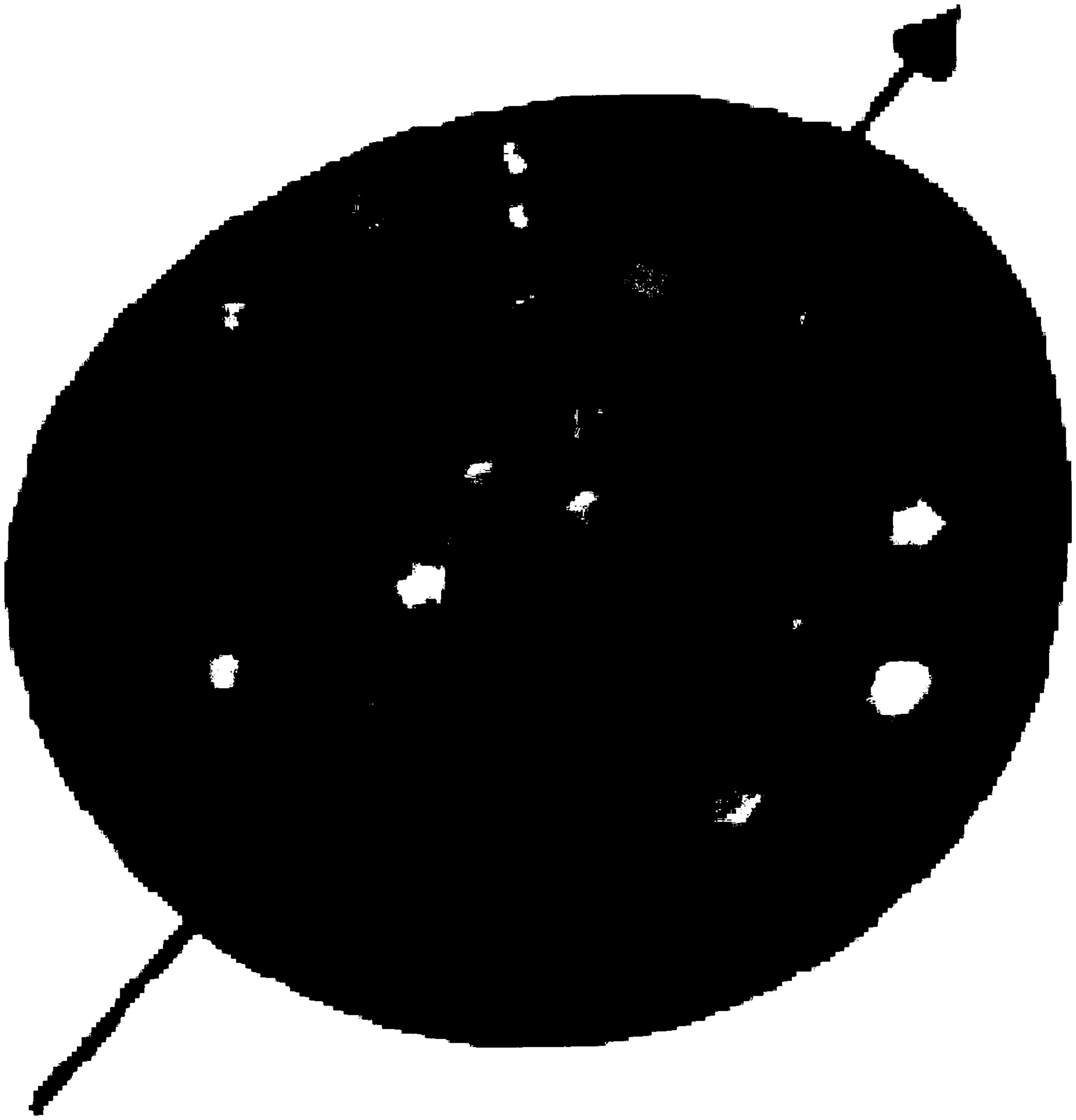

Nucleus

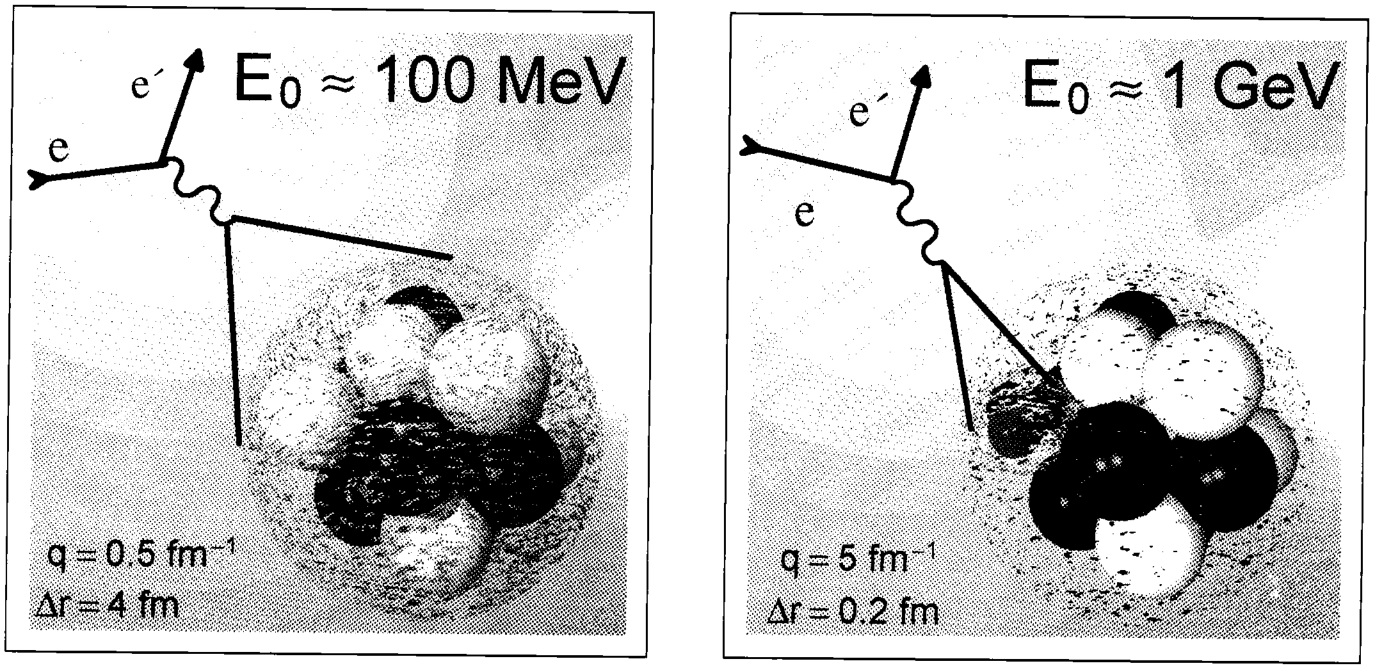

Nucleon

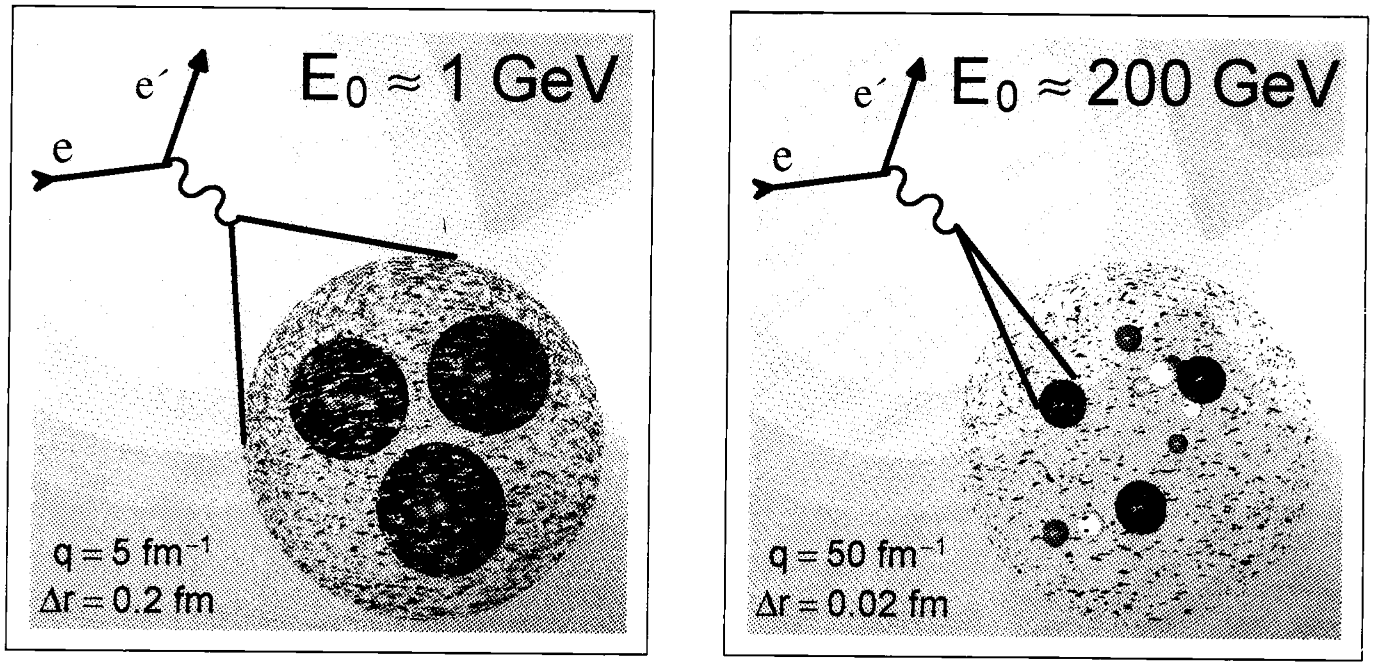

running coupling constant of the strong interaction

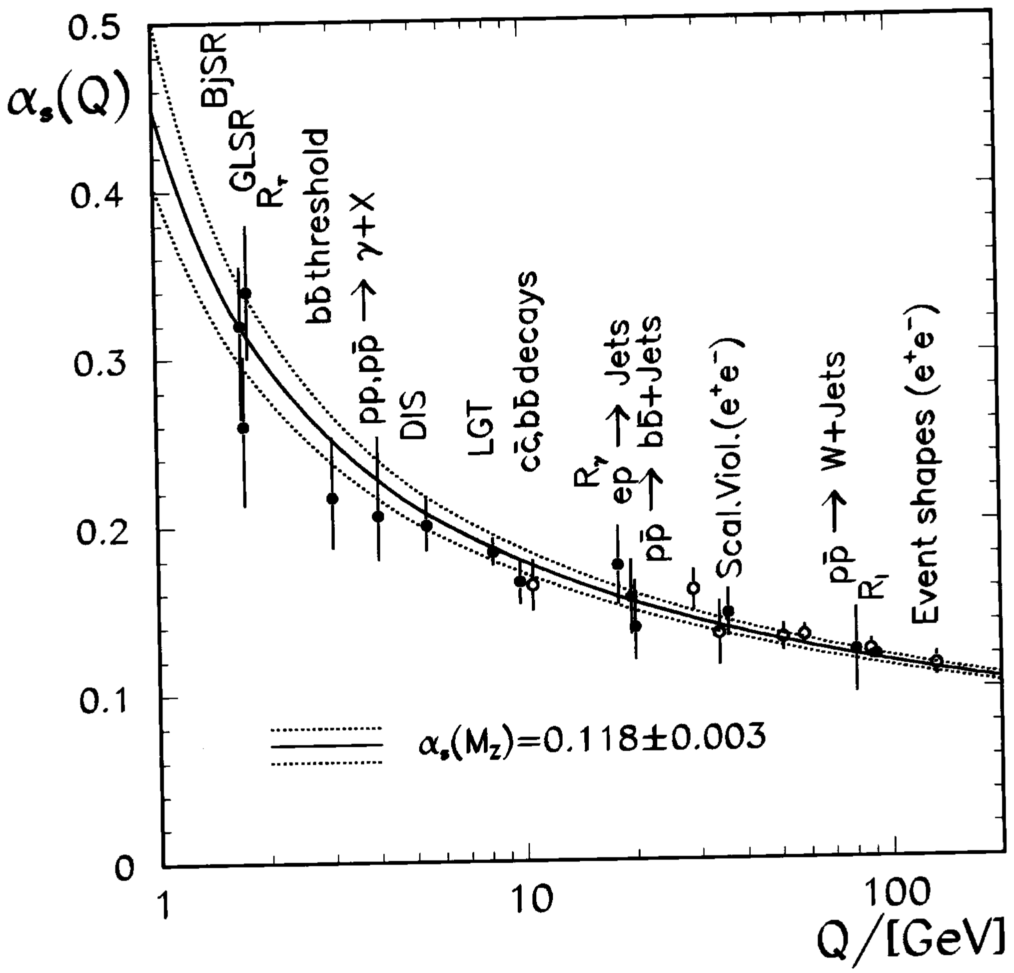

MAINZER MIKROTRON

SFB 443

Form factors of the nucleon

Elastic Formfactors

scattering of light:

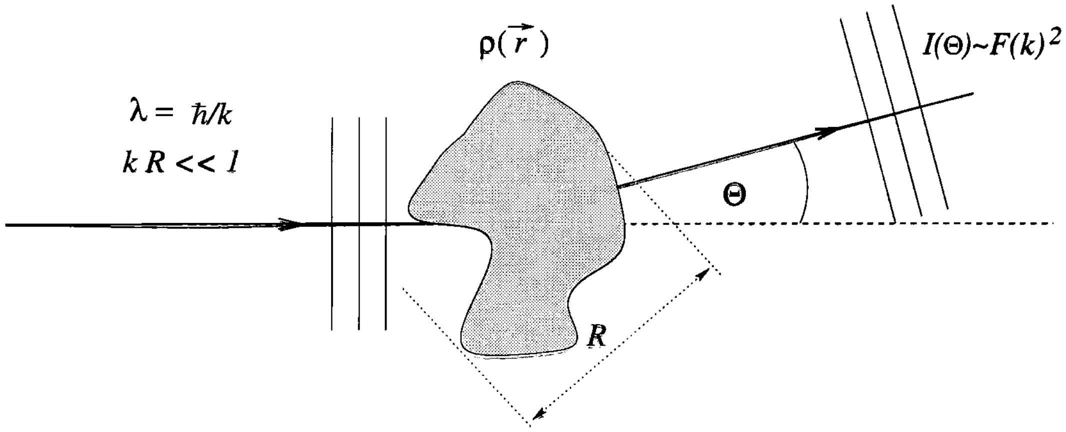

$$I(\Theta) = I_0 \cdot \left(\frac{d\sigma}{d\Omega}\right)_{Thompson} \cdot |F(\vec{k})|^2$$

$$F(\vec{k}) = \int \left(\rho(\vec{r}) \cdot e^{i\vec{k}\cdot\vec{r}}\right) d^3\vec{r}$$

elastic electron–nucleon–scattering:

$$\frac{d\sigma}{d\Omega} = \left(\frac{d\sigma}{d\Omega}\right)_{Mott} \cdot \left(\frac{G_E^2(Q^2) + \tau G_M^2(Q^2)}{1 + \tau} + 2\tau\, G_M^2(Q^2)\, \tan^2 \frac{\Theta}{2} \right)$$

$$Q^2 = \vec{q}^{\,2} - \omega^2; \quad \tau = Q^2/4\,M^2$$

4 formfactors : $G_{E,p}(Q^2)$, $G_{M,p}(Q^2)$

$G_{E,n}(Q^2)$, $G_{M,n}(Q^2)$

Measurement of $G_{E,n}$ in $\mathrm{D}(\vec{e}, e'\vec{n})p$

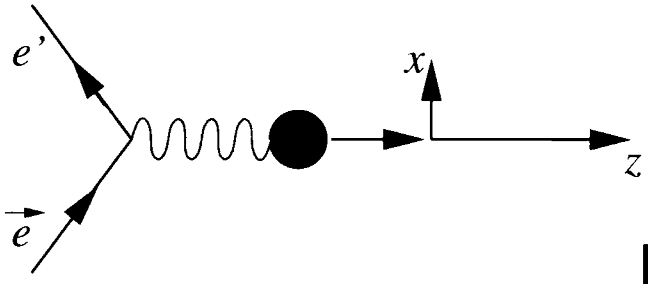

Asymmetry $A = P_e \mathcal{A}_{\text{eff}} P_t \sin \Phi_n$

$$\mathcal{P}_x = -hP_e \frac{aG_E G_M}{G_E^2 + bG_M^2}$$

$$\mathcal{P}_y = 0$$

$$\mathcal{P}_z = hP_e \frac{cG_M^2}{G_E^2 + bG_M^2}$$

Arnold, Carlson & Gross,
PR C **23** (1981), 363

LD_2 Target | Dipole Magnet | Front Wall | Rear Wall

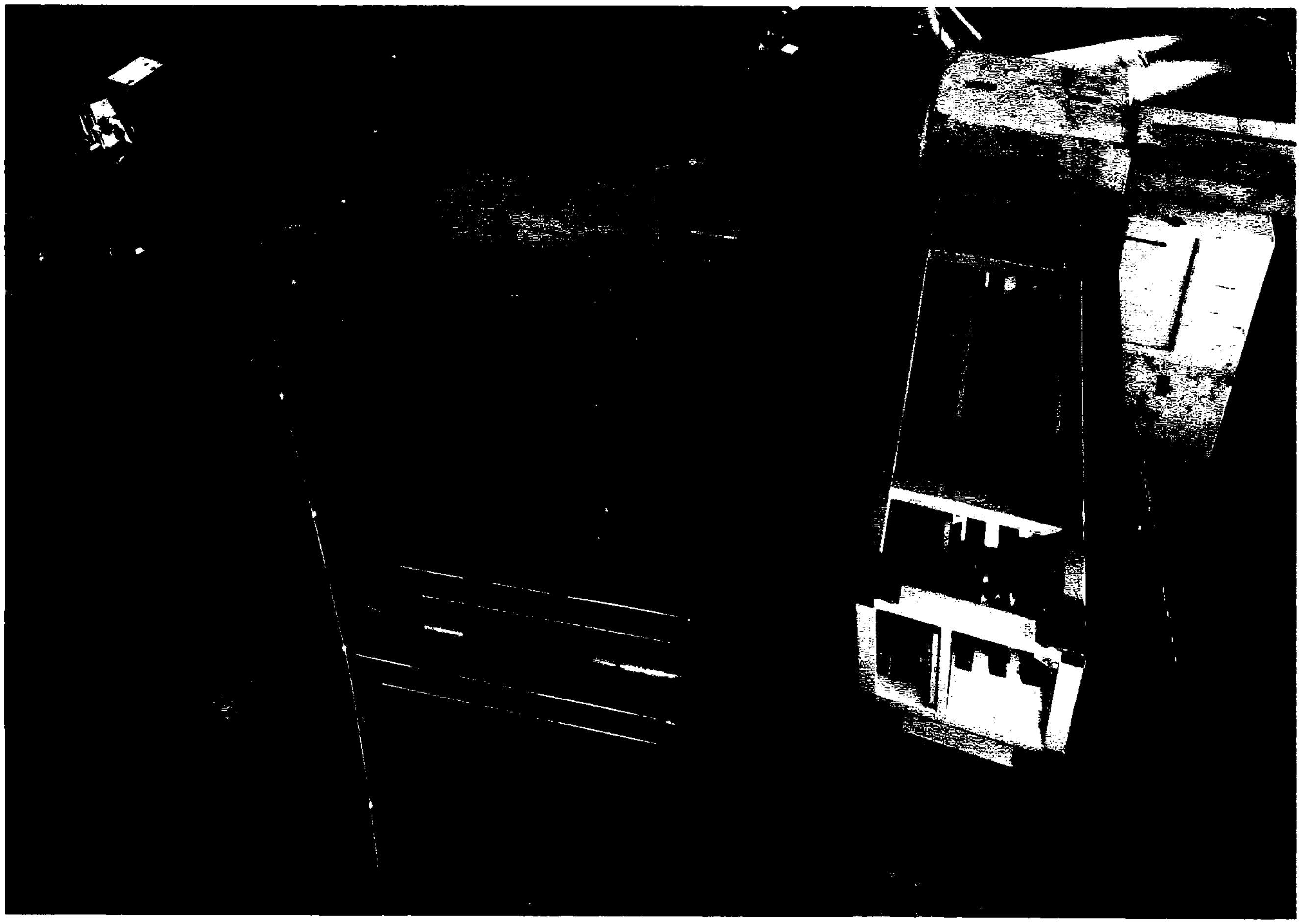

Method:
T. N. Taddeucci et al.,
NIM **A241** (1985), 448

Michael Seimetz

A1 Three Spectrometer Setup

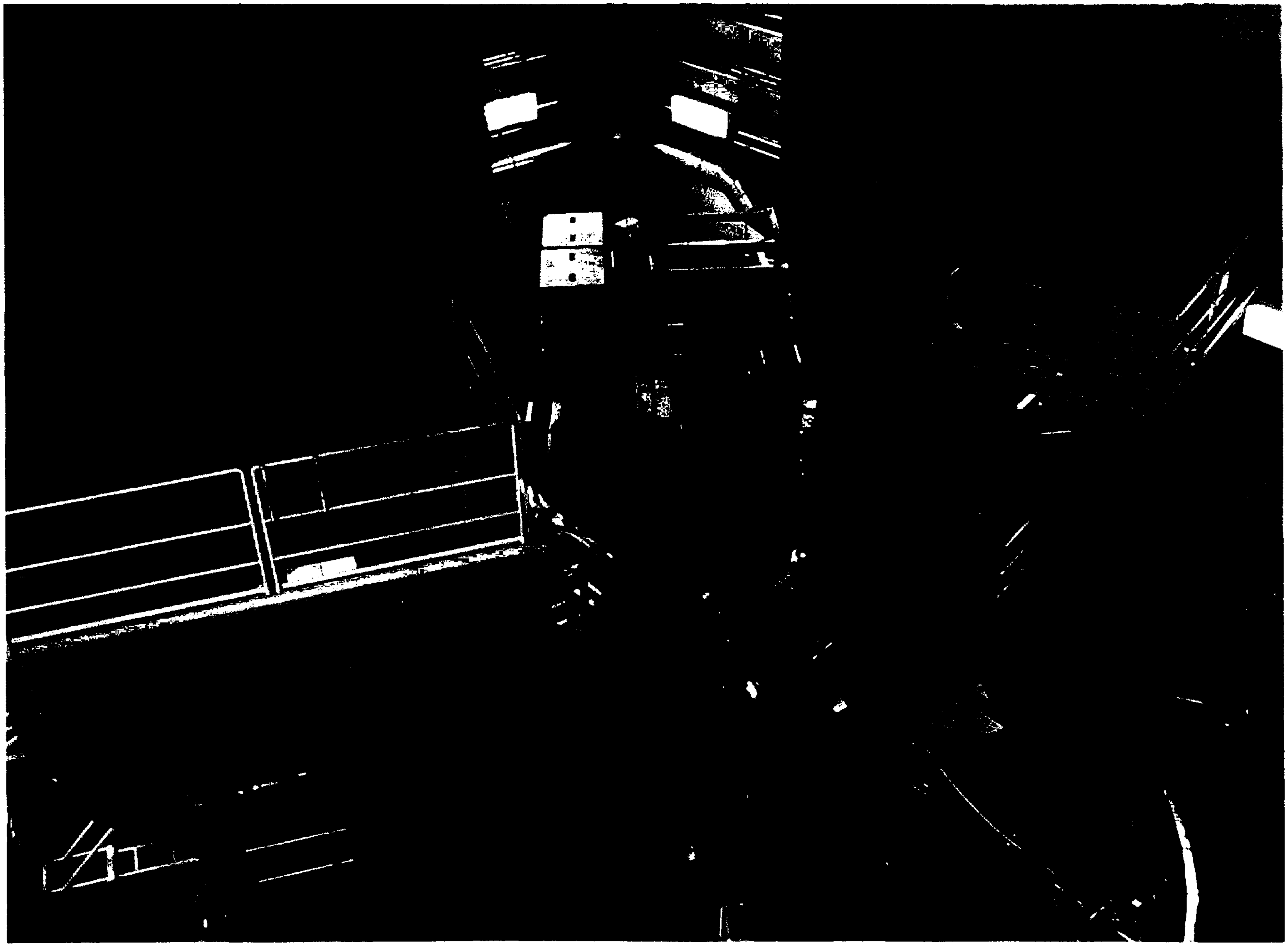

Neutron Polarimeter, Rear Wall

24 scintillator bars, $180 \times 20 \times 10$ cm^3
$\Rightarrow$ high background rates
$\Rightarrow$ avoid direct target view

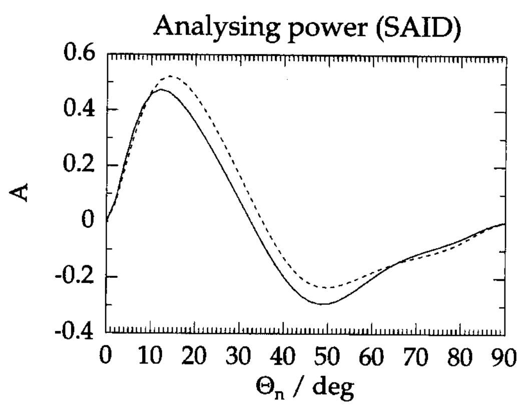

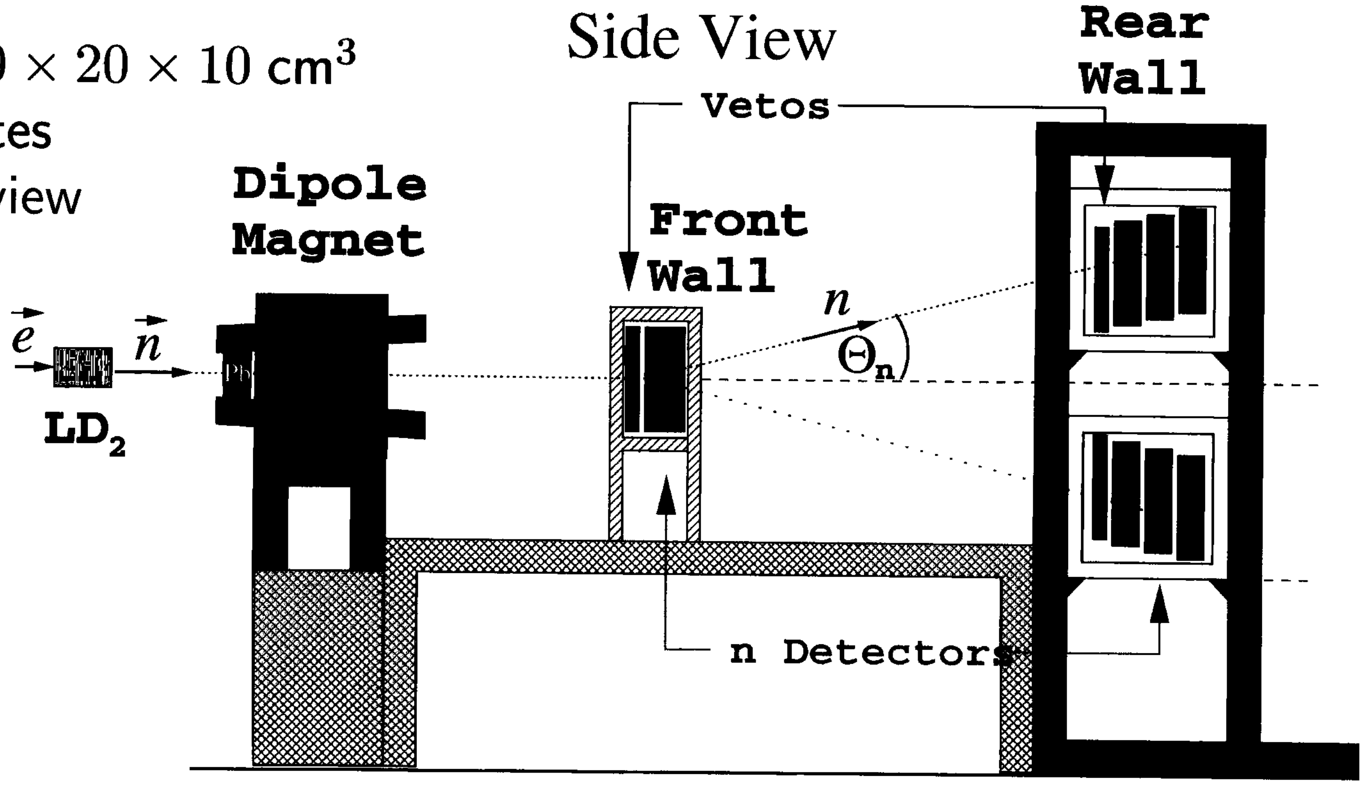

Spin Precession Method

Mixing of two spin components by precession of neutron spin in magnetic field,

$$\mathcal{P}_t(\chi) = \mathcal{P}_x \cos(\chi) + \mathcal{P}_z \sin(\chi) =: \mathcal{P}_0 \sin(\chi - \chi_0)$$

(M. Ostrick et al., PRL **83** (1999) 276)

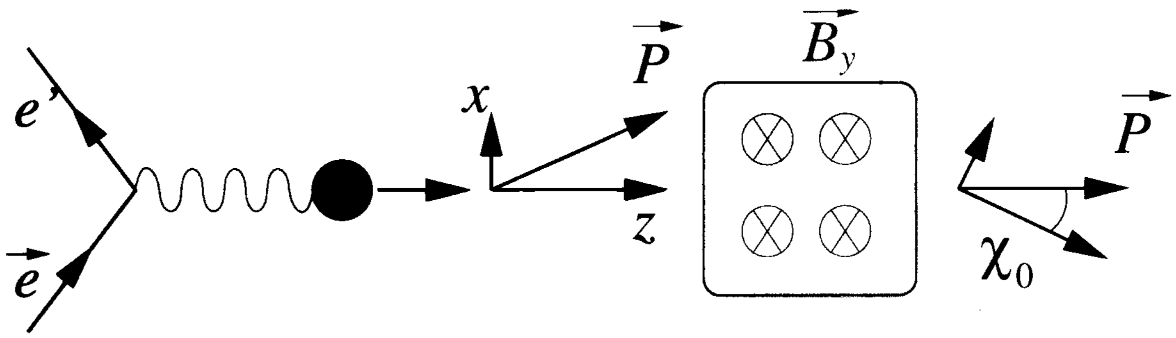

$$\tan \chi_0 = \frac{\mathcal{P}_x}{\mathcal{P}_z} = \frac{A_x}{A_z} = \frac{a\,\mathcal{A}_{\text{eff}} P_e}{c\,\mathcal{A}_{\text{eff}} P_e} \cdot \frac{G_{E,n}}{G_{M,n}} \quad .$$

Asymmetries

Φ_n distributions:

$h = -1,\ \Phi_n > 0 \qquad h = +1,\ \Phi_n > 0$

$h = -1,\ \Phi_n < 0 \qquad h = +1,\ \Phi_n < 0$

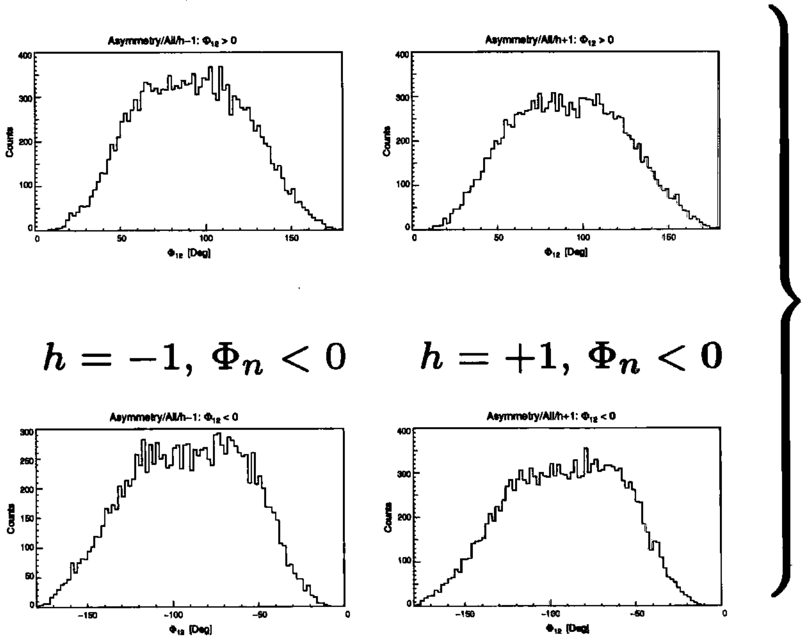

$$A(\Phi_n) = \frac{\sqrt{N^+(\Phi_n)N^-(\Phi_n+\pi)} - \sqrt{N^+(\Phi_n+\pi)N^-(\Phi_n)}}{\sqrt{N^+(\Phi_n)N^-(\Phi_n+\pi)} + \sqrt{N^+(\Phi_n+\pi)N^-(\Phi_n)}}$$

Asymmetry

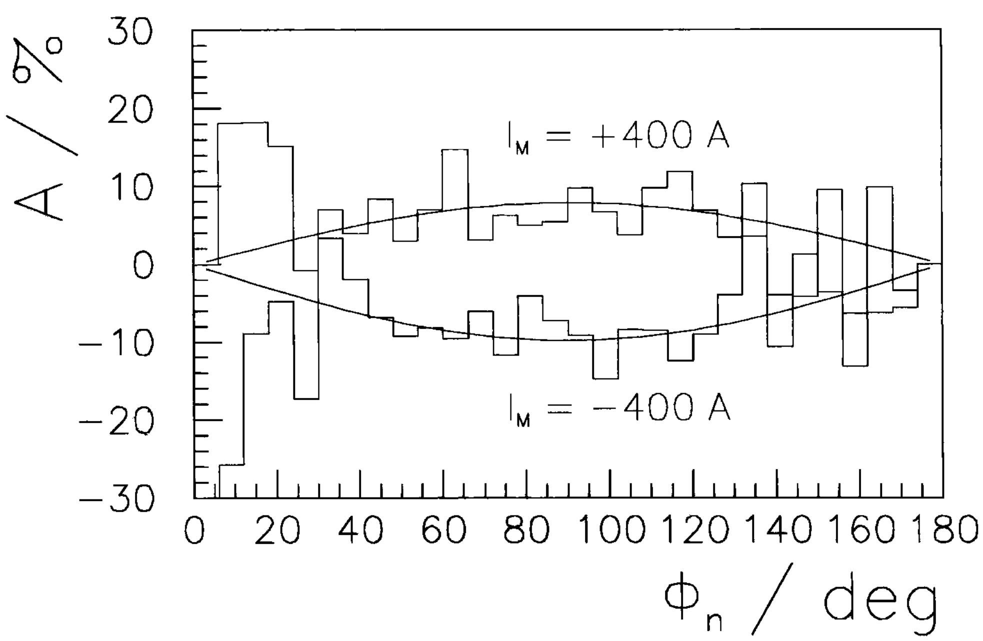

Asymmetries

Plot asymmetries as function of spin precession angle χ

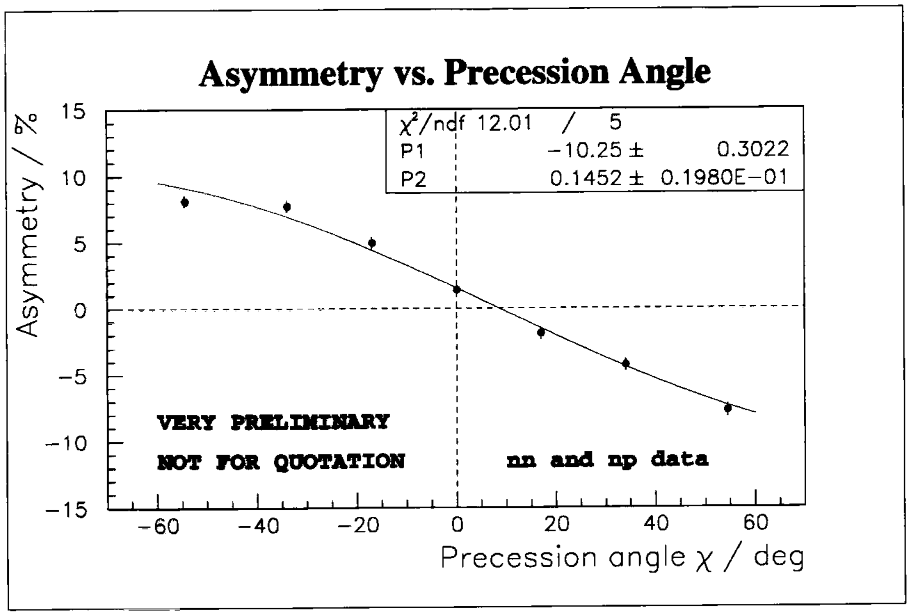

electric form factor of the neutron

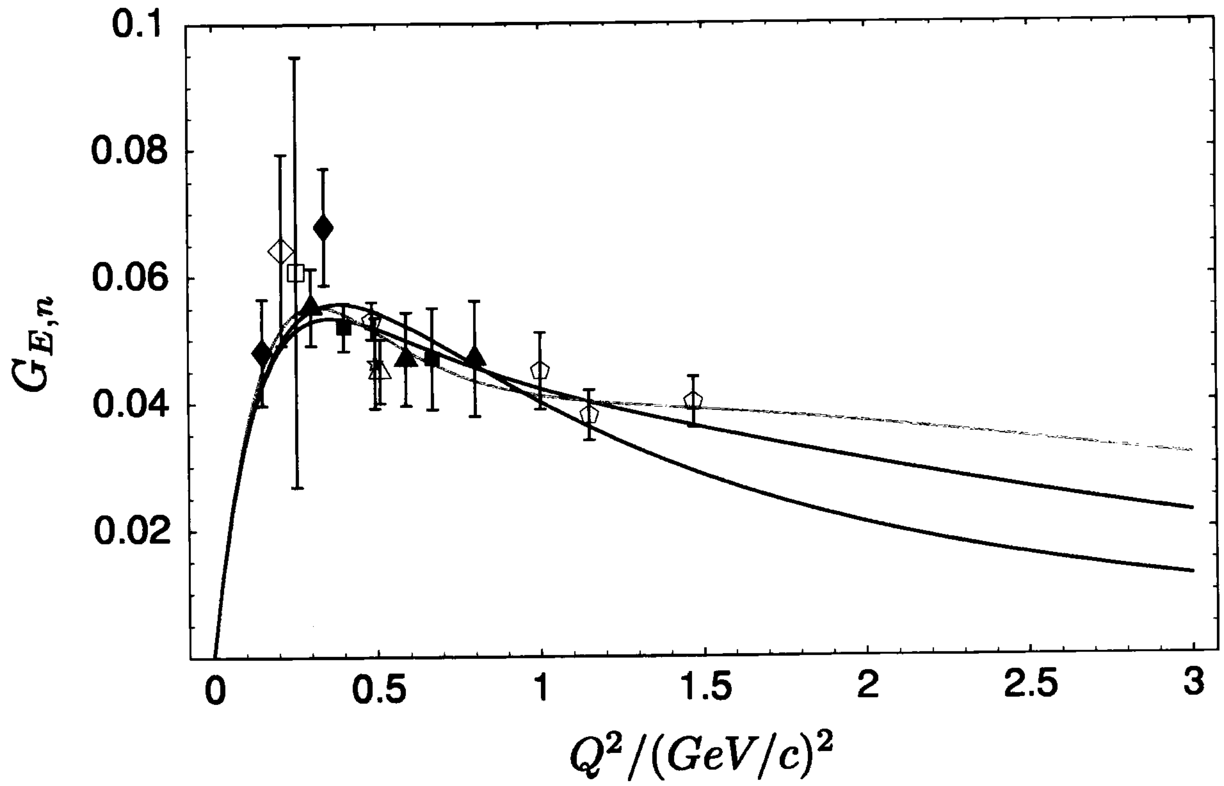

electric charge distribution of the neutron

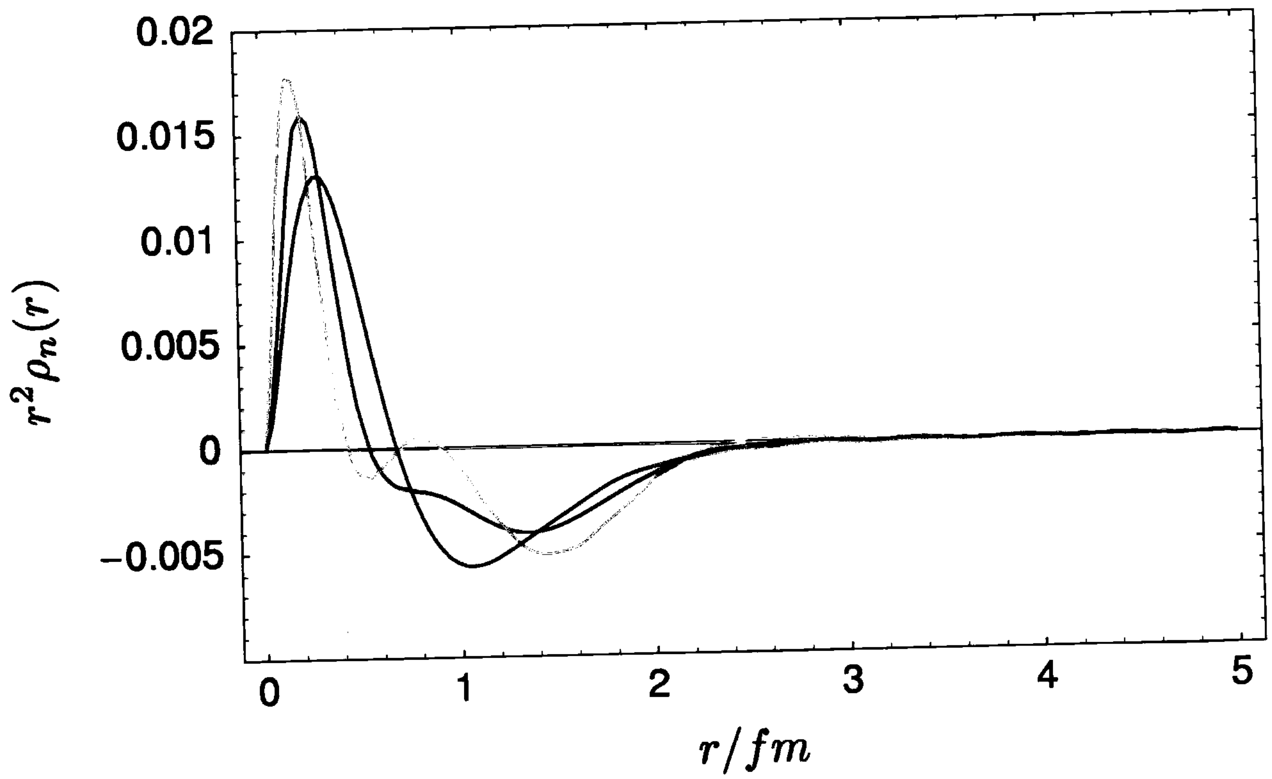

Form factors of the nucleon

fit with 2 dipole shapes and 1 “Gauss”

form factors | form factor / standard dipole

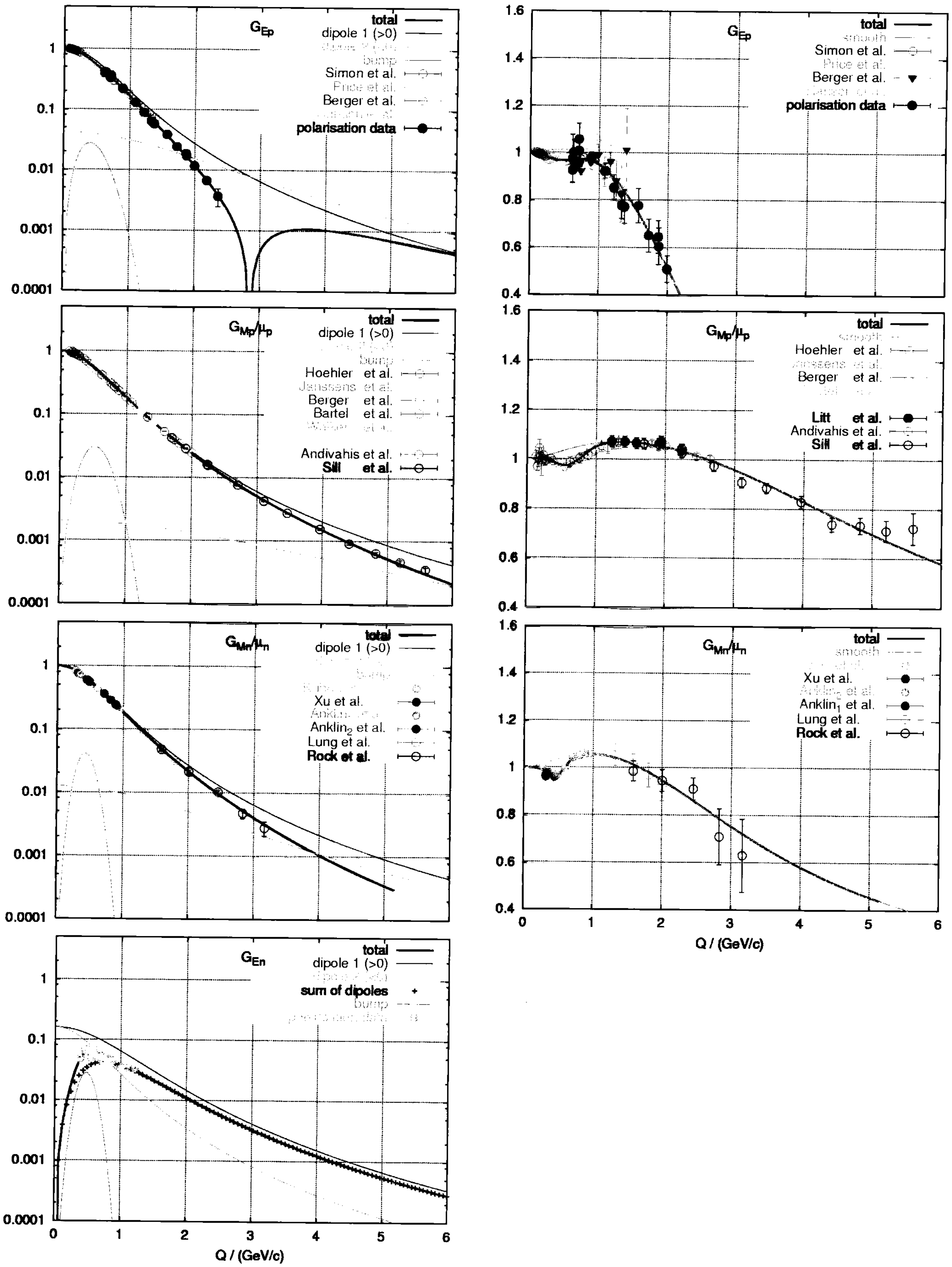

measurement minus smooth fit ≡ 2 dipole shapes plus "Gauss"

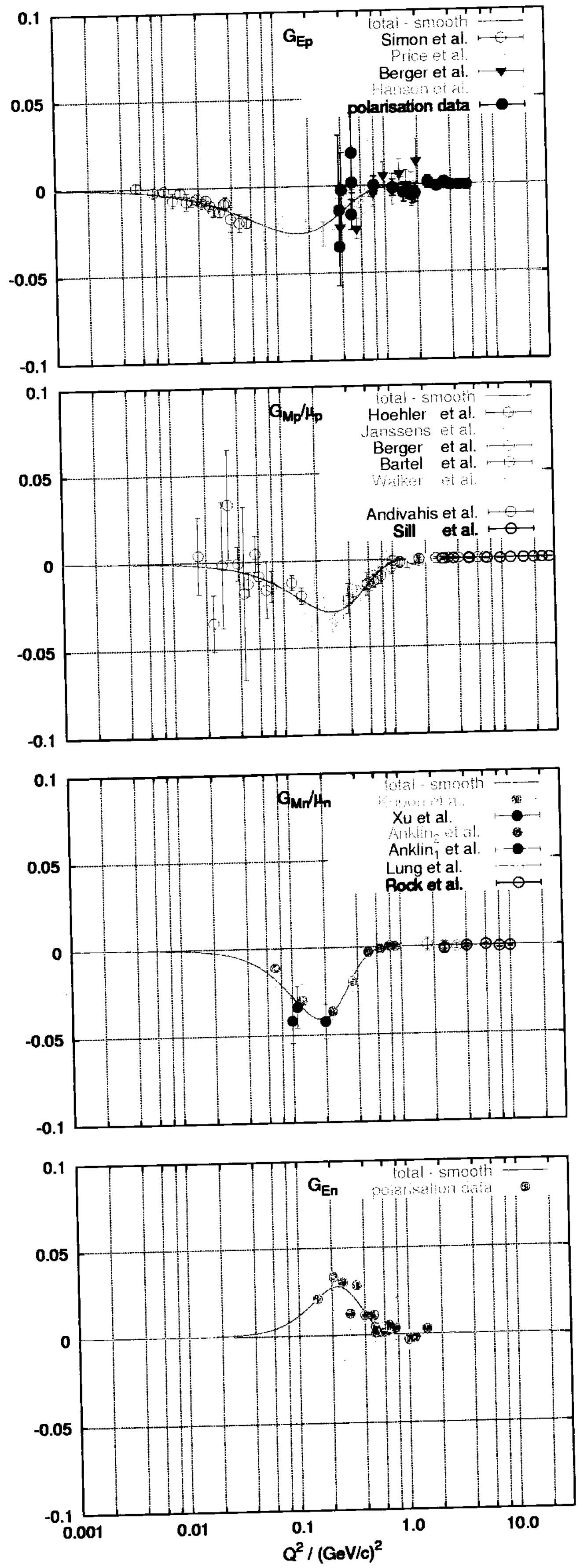

SFB 443

Measurement of the π^+ polarizability in the $\gamma p \to \gamma' \pi^+ n$ reaction.

Meaning of the polarizability of a composed system

electric polarizability α

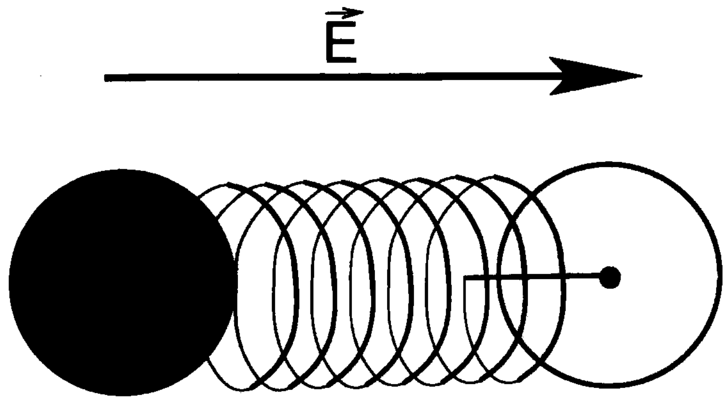

spring

$$\vec{p}_{el} := q\delta = q\frac{q}{D}\vec{E} =: \varepsilon_0 \alpha \vec{E} \quad \curvearrowright \quad \alpha = \frac{1}{\varepsilon_0}\frac{q^2}{D} = 4\pi\hbar c\,\alpha_{QED}\frac{\zeta^2}{D}; \quad D = \frac{G}{4}\frac{r^4}{R^3}$$

$$\alpha_{spring} = \hbar c\frac{\alpha_{QED}}{G}16\pi\frac{R^3}{r^4}\zeta^2$$

$$\boxed{\alpha_{spring} \propto \frac{\alpha_{QED}}{\alpha_{spring}} length^3}$$

Experimental situation

Experiments	$\alpha_{\pi^\pm}/10^{-4}\text{fm}^3$	$\alpha_{\pi^0}/10^{-4}\text{fm}^3$
$\pi^- Z \to \gamma\pi^- Z$, Serpukhov (1983)	$6.8 \pm 1.4 \pm 1.2$	
$\gamma p \to \gamma\pi^+ n$, Lebedev Phys.Inst. (1984)	20 ± 12	
D. Babusci *et al.* (1992)		
$\gamma\gamma \to \pi^+\pi^-$: PLUTO (1984)	$19.1 \pm 4.8 \pm 5.7$	
DM 1 (1986)	17.2 ± 4.6	
DM 2 (1986)	26.3 ± 7.4	
MARK II (1990)	2.2 ± 1.6	
$\gamma\gamma \to \pi^0\pi^0$: Crystal Ball (1990)		$\pm 0.69 \pm 0.11$
F. Donoghue, B. Holstein (1993)		
$\gamma\gamma \to \pi^+\pi^-$: MARK II	$2.7 \pm ?$	
$\gamma\gamma \to \pi^0\pi^0$: Crystal Ball		$-0.5 \pm ?$
	$(\alpha+\beta)_{\pi^0}/10^{-4}\text{fm}^3$	$(\alpha-\beta)_{\pi^0}/10^{-4}\text{fm}^3$
A. Kaloshin, V. Serebryakov (1994) $\gamma\gamma \to \pi^0\pi^0$: Crystal Ball	1.00 ± 005	-0.6 ± 1.8
L. Fil'kov, V. Kashevarov (1999) $\gamma\gamma \to \pi^0\pi^0$: Crystal Ball	0.98 ± 003	-1.6 ± 2.2

Theoretical predictions

- **chiral perturbation theory**
  - ⋆ $(\alpha+\beta)_{\pi^+} = 0$ in leading order $O(p^4)$
    $(\alpha+\beta)_{\pi^+} = (0.3\pm0.1)\times10^{-4}\mathrm{fm}^3$ in order $O(p^6)$
  - ⋆ $(\alpha-\beta)_{\pi^+} \approx 5.4\times10^{-4}\mathrm{fm}^3$ one loop (Bijens, Cornet, 1988; Danoghue, Holstein 1989; Belluci, Gasser, Sainio, 1994)
    $(\alpha-\beta)_{\pi^+} = (4.4\pm1.0)\times10^{-4}\mathrm{fm}^3$ two loops (Bürgi, 1997)
- **Nambu-Jona-Lasino model**
  $\alpha = -\beta = (3.0\pm0.6)\times10^{-4}\mathrm{fm}^3$; $(\alpha-\beta)_{\pi^+} = (6.0\pm0.8)\times10^{-4}\mathrm{fm}^3$
- **Dispersion relations**
  $(\alpha-\beta)_{\pi^+} = (10.3\pm1.9)\times10^{-4}\mathrm{fm}^3$ **(Lev Fil'kov, Kashevarov, 1999)**
- **non linear σ model**
  $(\alpha-\beta)_{\pi^+} = 20\times10^{-4}\mathrm{fm}^3$ **(Bernard, Hiller, Weise, 1988)**
- **Dubna quark confinement model**
  $(\alpha-\beta)_{\pi^+} = 7.05\times10^{-4}\mathrm{fm}^3$ **(Ivanov, Mizutani, 1992)**

Basic idea for measuring the π^+ polarizability.

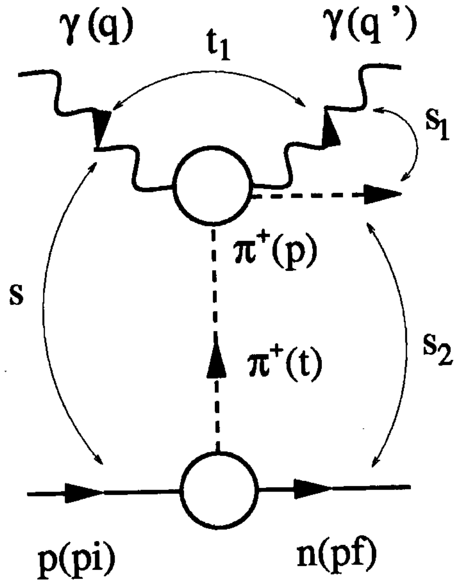

$$
\begin{aligned}
s &= (p_1+k_1)^2 = m_p^2 + 2m_pE_\gamma \\
t &= (p_2-p_1)^2 = (m_n-m_p)^2 - 2m_p(E_n-m_n) \\
t_1 &= (k_2-k_1)^2 = -2E_\gamma E_{\gamma'}(1-\cos\theta_{\gamma\gamma'}) \\
s_1 &= (k_2+q_2)^2 = m_\pi^2 + 2E_{\gamma'}(q_{20} - \mid \vec{q}_2 \mid \cos\theta_{\gamma\pi^+}) \\
s_2 &= (p_2+q_2)^2 = s + t_1 - 2m_pE_{\gamma'} \\
z &= cos\theta_{\gamma\gamma'}^{cm}
\end{aligned}
$$

$$
\frac{d\sigma_{\gamma\pi}}{d\Omega} = \left(\frac{d\sigma_{\gamma\pi}}{d\Omega}\right)_B - \frac{e^2}{4\pi} \frac{m_\pi^3(s_1-m_\pi^2)^2}{4s_1^2[(s_1+m_\pi^2)+(s_1-m_\pi^2)z]} \times \left\{(1-z)^2(\alpha_{\pi^\pm}-\beta_{\pi^\pm}) + \frac{s_1^2}{m_\pi^4}(1+z)^2(\alpha_{\pi^\pm}+\beta_{\pi^\pm})\right\}
$$

background reaction

only backward direction of γ detection is interesting and covered (TAPS)

$\curvearrowright$ background

$$\gamma p \rightarrow \pi^0 \pi^+ n \rightarrow \gamma' \gamma \pi^+ n \rightarrow \gamma' \pi^+ n$$

$\downarrow$

lost

choice of detector setup supresses this abundant reaction,
Monte Carlo simulations show that with analysis methods:

- optimized cut $\curvearrowright$ background $\leqslant 3\%$
- constrained fits $\curvearrowright$ background $\leqslant 10\%$

Experimental Set-up

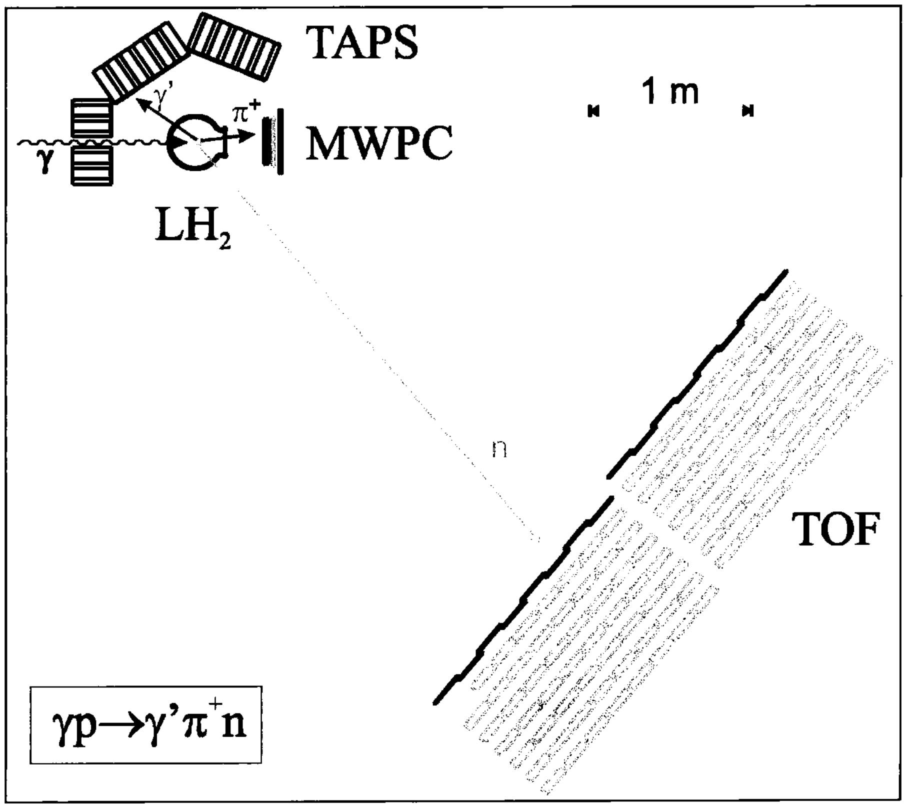

TAPS:
A: 192 BaF2, θ=68°
B: 192 BaF2, θ=124°
C: 144 BaF2, θ=180°
MWPC:
4 planes×128 wires, θ=0°
TOF:
111 bars, 300×20×5 cm^3, θ=40°
16 veto bars 300×22×1cm^3
Target:
LH_2 11 cm long , 3 cm dia.

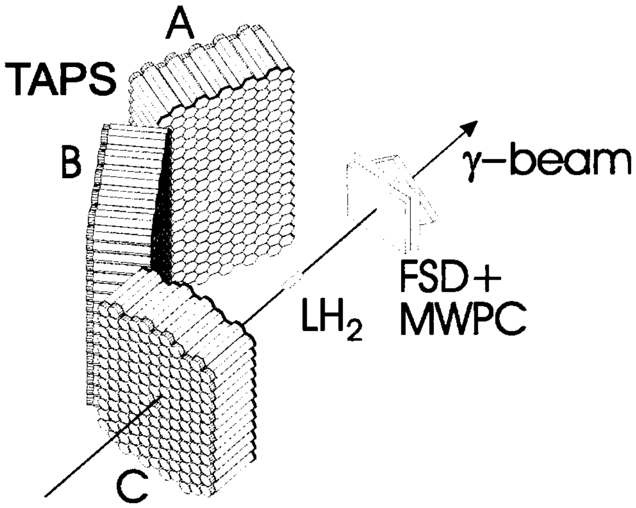

Differential cross section

$\gamma\ p \longrightarrow \gamma'\ \pi^+\ n$

$537\ \text{MeV} < E_\gamma < 817\ \text{MeV}$

$140^\circ < \theta^{cm}_{\gamma\gamma'} < 180^\circ$

$1.5\ \mu^2 < s_1 < 5\ \mu^2$

Insensitive to pion polarizability!

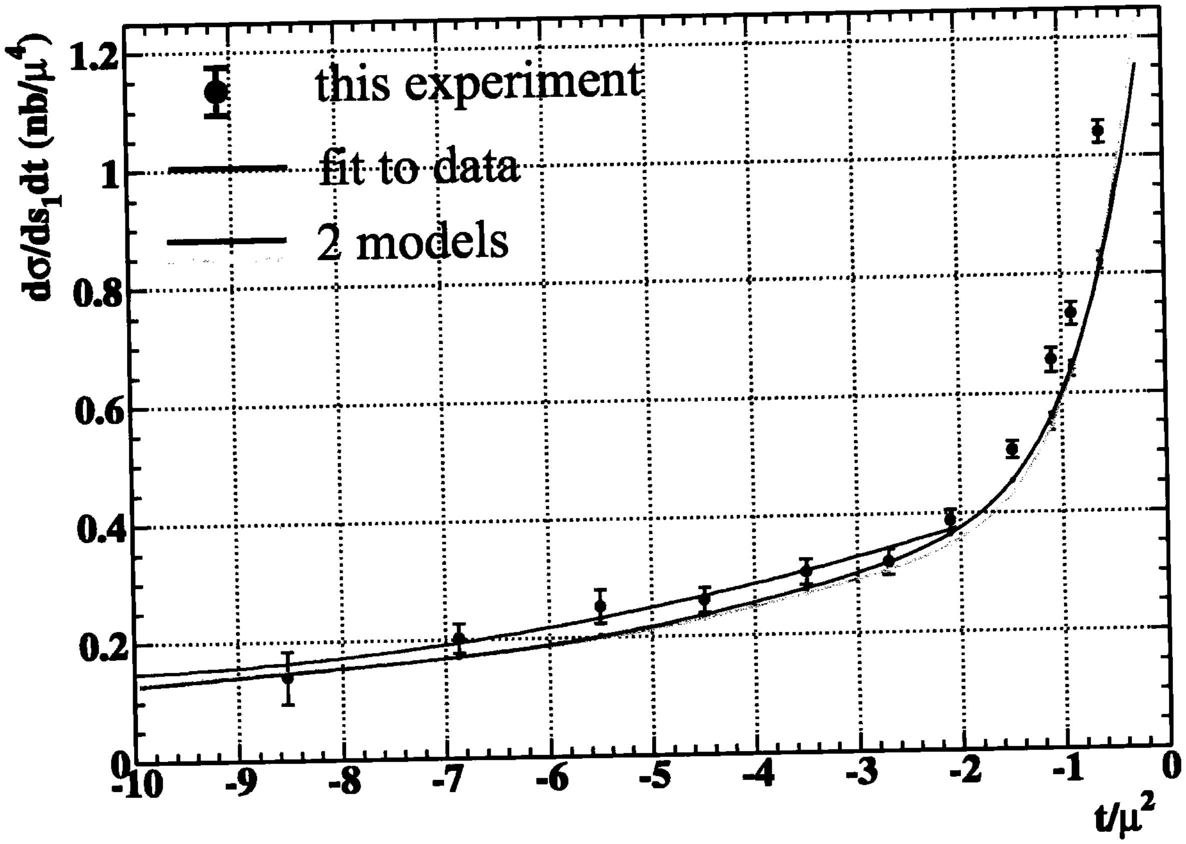

Pion Polarizability

$\gamma\ p \rightarrow \gamma'\ \pi^+\ n$

cross section for: $140^\circ < \theta_{\gamma\gamma'}^{cm} < 180^\circ$

$-12\ \mu^2 < t < -2\ \mu^2$

$5\ \mu^2 < s_1 < 15\ \mu^2$

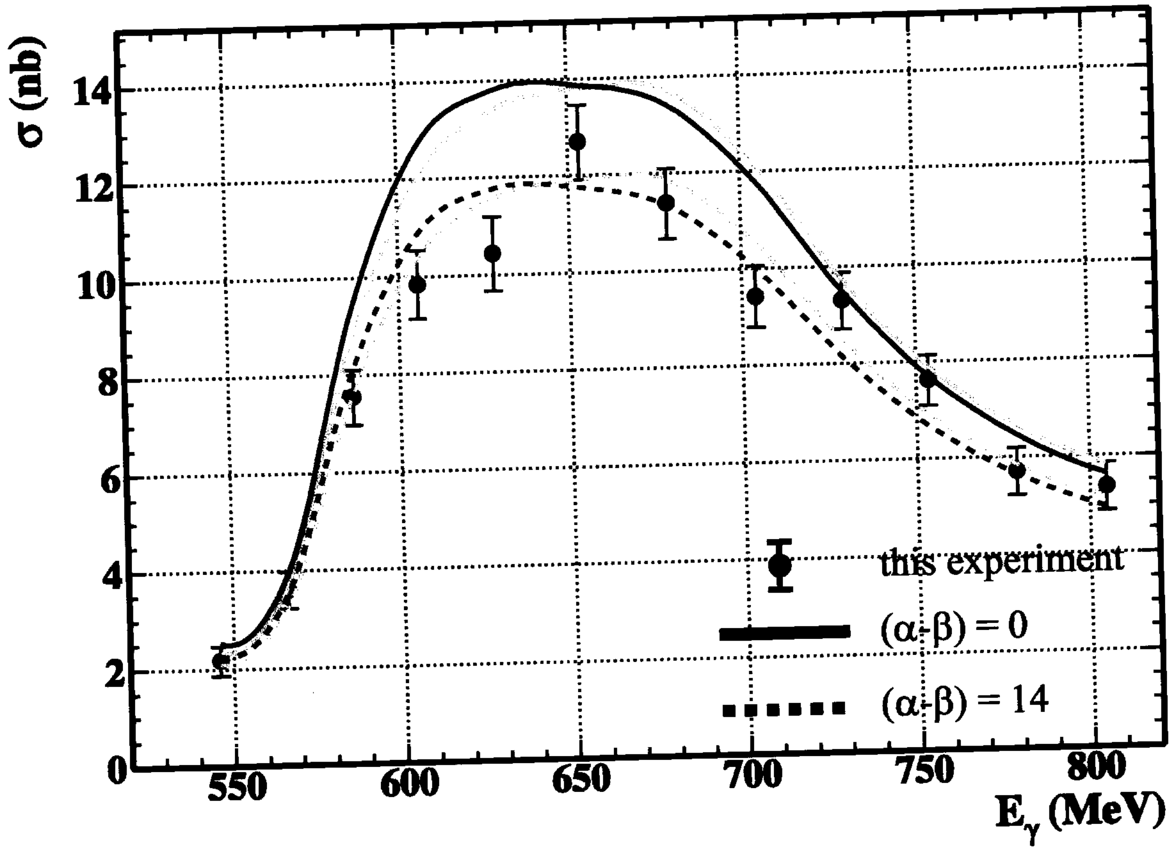

Model 2: Fil'kov $(\alpha-\beta)=(11.1\pm1.4\pm2.8)\times10^{-4}\ \text{fm}^3$

Conclusions

Final result for pion polarizabilty $(\alpha-\beta)_{\pi^+}$:

$$(\alpha-\beta)_{\pi^+} = (11.6 \pm 1.5_{stat} \pm 3.0_{syst} \pm 0.5_{model}) \times 10^{-4}\mathrm{fm}^3$$

deviates by 2 standard deviations from the

Chiral Perturbation Theory **result;**

significant deviation, but a real problem?

Explanations:

- **“off-shell-pion”**
  the initial pion is virtual, the final is the asymptotic pion
  replace point like initial pion by form factor $\curvearrowright$ discrepancy increases
- **Chiral Perturbation Theory fails**
  expansion for small external momenta, but how small?
  deviations manifest if $\lambda_\pi \gtrapprox \lambda_{\gamma^*}$, i.e. if spatial size of pion is resolved
- **modification of pion cloud picture**
  pion cloud $\equiv$ transitional layer between superconductor (QCD vacuum) and normal conductor (interior of hadron, confined quarks and gluons)?

ranges of physics

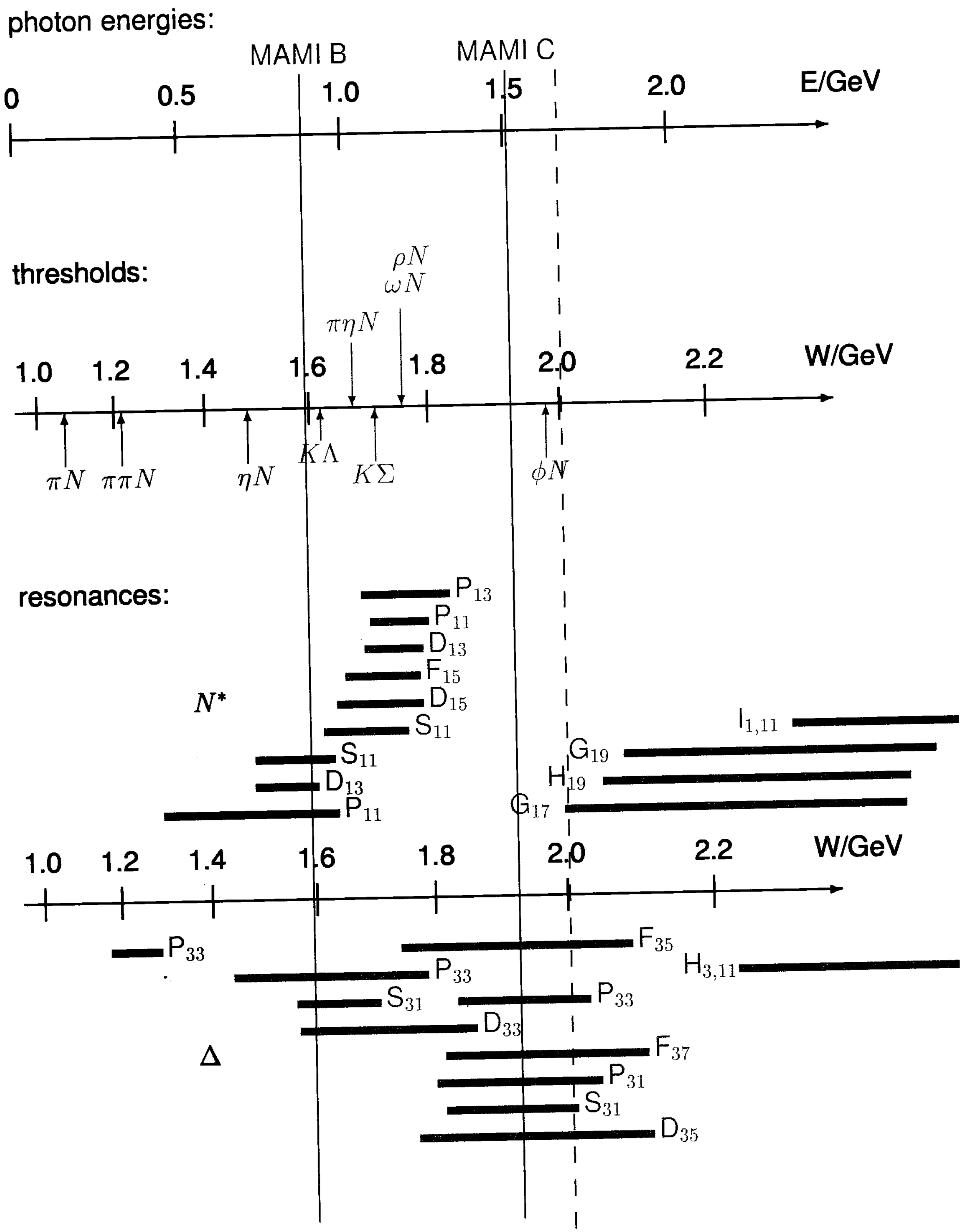

The MAMI accelerator

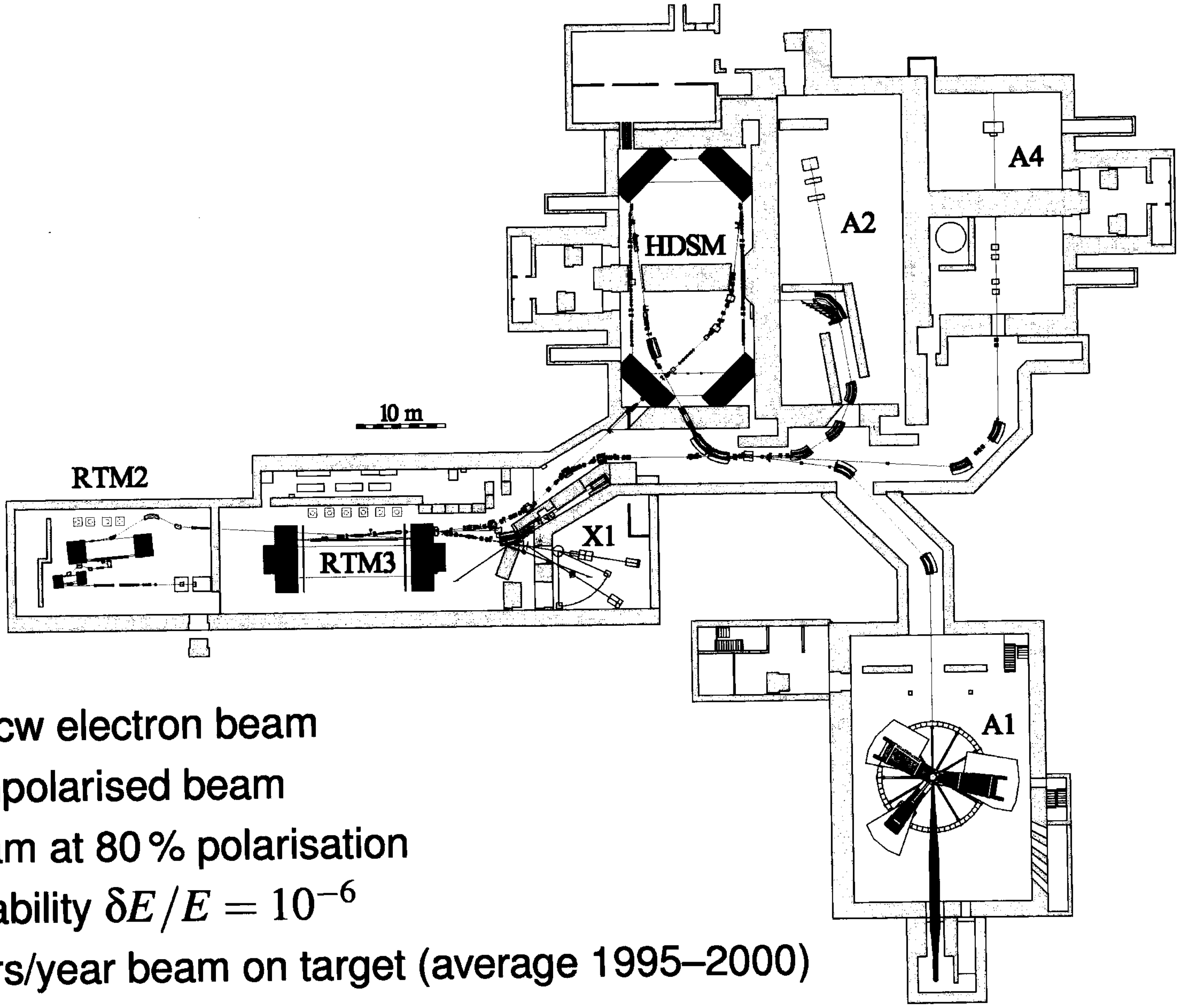

- 855 MeV cw electron beam
- 100 μA unpolarised beam
- 30 μA beam at 80 % polarisation
- energy stability $\delta E/E = 10^{-6}$
- 5500 hours/year beam on target (average 1995–2000)

MAMI C

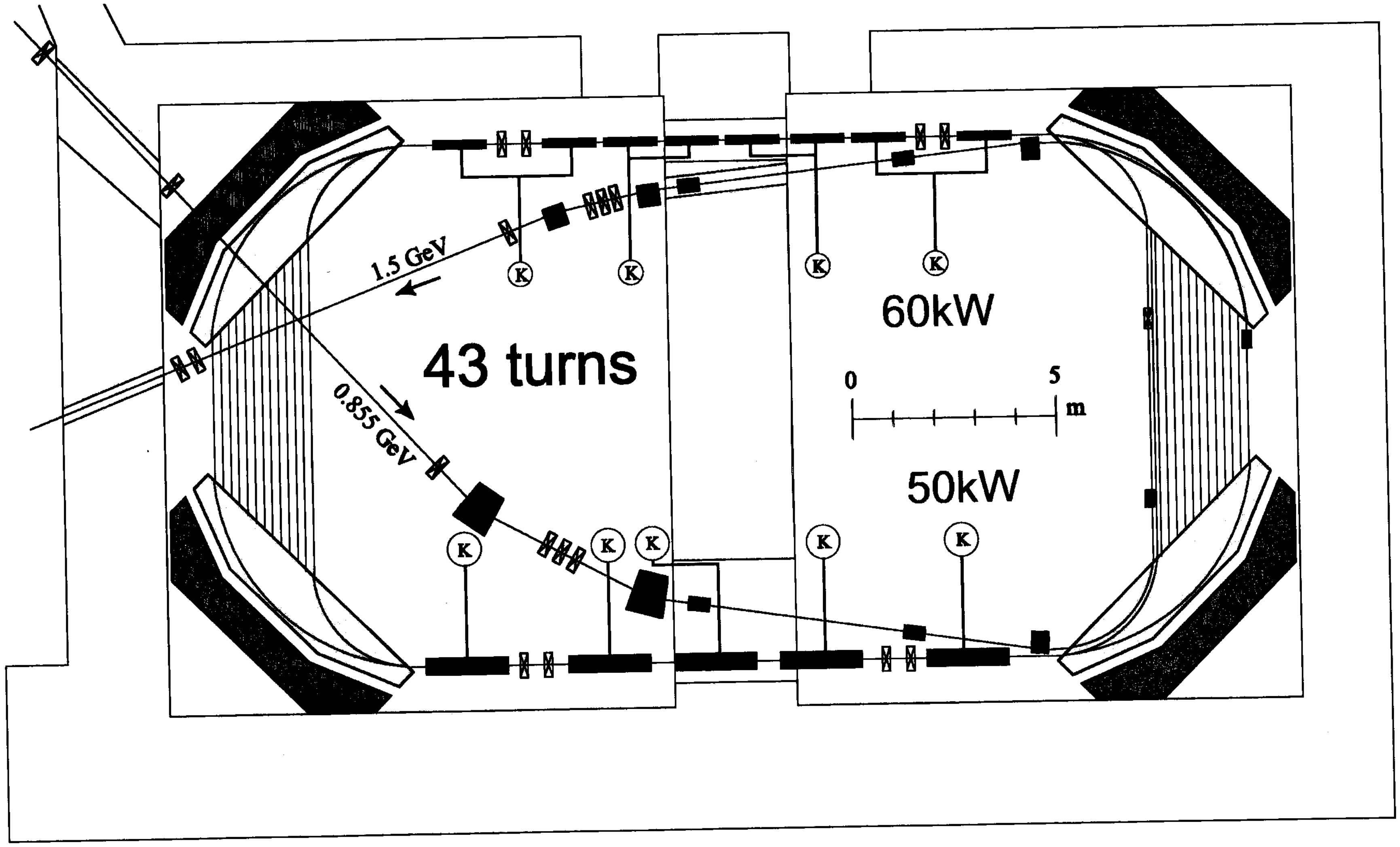

MAMI collaborations and their experimental equipment

- **A1 collaboration**
  - ⋆ 3-Spectrometer-Set-up
  - ⋆ π Short Orbit Spectrometer
  - ⋆ neutron polarimeter and detectors
  - ⋆ $^3\overrightarrow{He}$ target
  - ⋆ KAOS Kaon short orbit Spectrometer
- **A2 collaboration**
  - ⋆ Photon-Tagger
  - ⋆ DAPHNE, TAPS, etc.
  - ⋆ Crystal Ball
  - ⋆ $\vec{p}$ target
- **A4 collaboration**
  - ⋆ granulated Cherenkov detector
  - ⋆ high power LH_2 target

KAOS @ A1

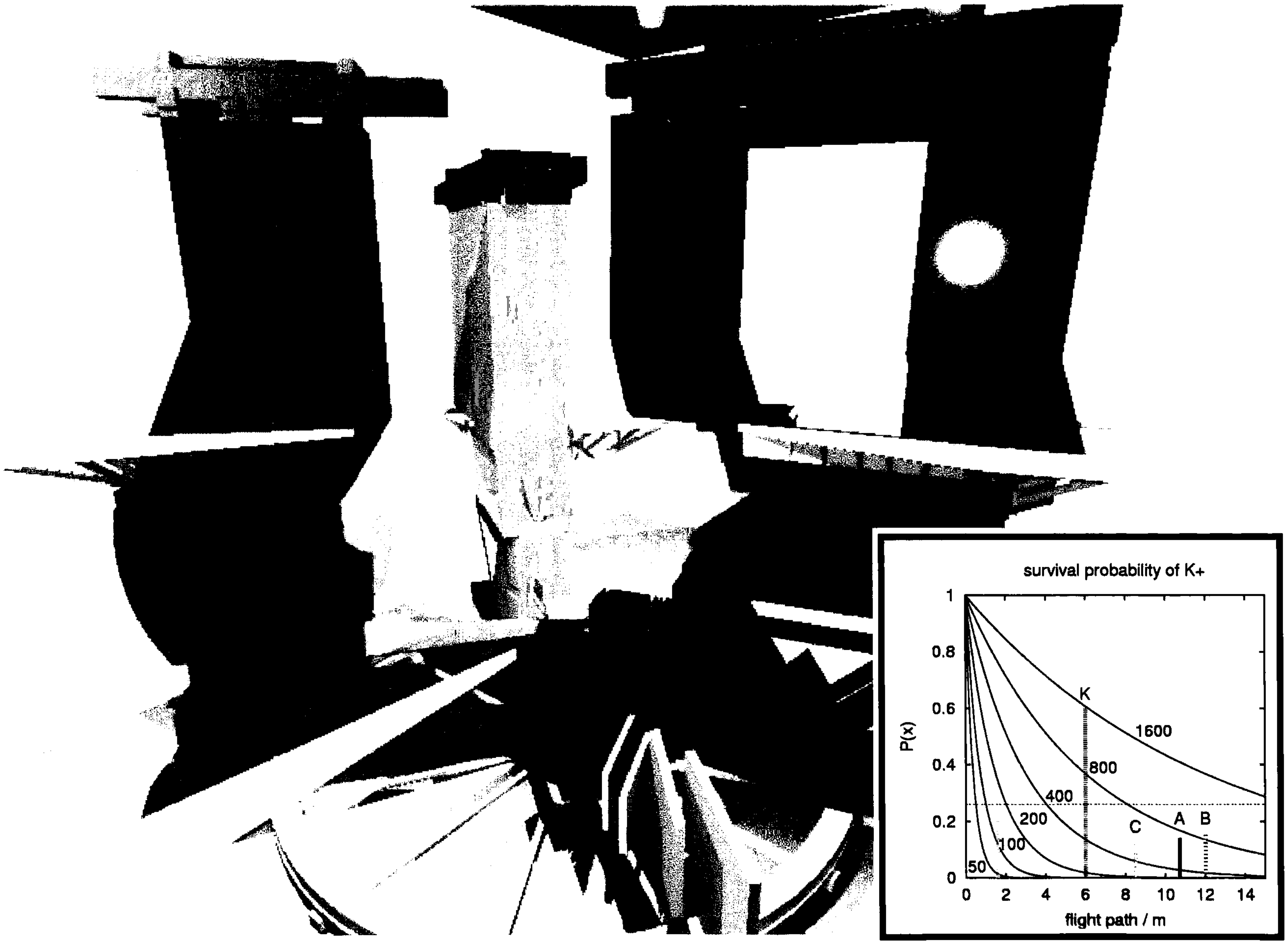

survival probability of K+
P(x)
flight path / m
1
0.8
0.6
0.4
0.2
0
0
2
4
6
8
10
12
14
K
1600
800
400
200
100
50
C
A
B

Crystal Ball and TAPS at MAMI

TAPS
510 BaF_2 detectors
max. kinetic energy
$\pi^{\pm}$: 180 MeV
$K^{\pm}$: 280 MeV
p : 360 MeV

Crystal Ball
672 NaJ detectors
max. kinetic energy
$\mu^{\pm}$: 233 MeV
$\pi^{\pm}$: 240 MeV
$K^{\pm}$: 341 MeV
p : 425 MeV

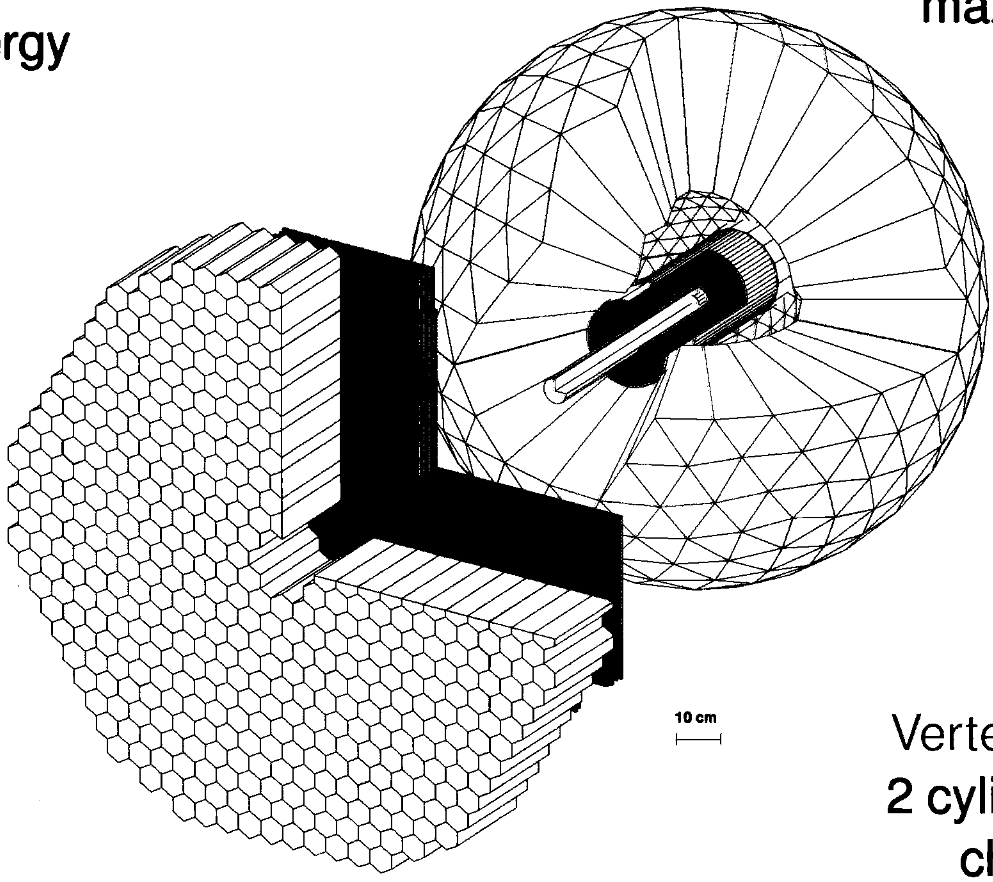

Vertex detectors
2 cylindrical wire chambers
480 wires, 320 strips

24 thin plastic counters
particle identifcation

Physics Program at MAMI

- MAMI B ($180\, MeV < E < 885\, MeV$) : from 1992 to 2005 and beyond
- MAMI C ($180\, MeV < E \lesssim 1500\, MeV$) : starting 2005

1. **Structure of the Nucleon**
   - form factors G_E^p, G_E^n, G_A
   - polarizabilities at $Q^2 = 0$ and $Q^2 > 0$
   - spin structure
   - nucleon resonances in selective decay channels
     ⋆ $\gamma\, p \rightarrow \Delta\, \gamma_{internal\ decay} \rightarrow p\, \pi^0\, \gamma$ $\curvearrowright$ magnetic moment of $\Delta(1232)$
     ⋆ Roper resonance

2. **Mesonic Structure of the Nucleon**
   - threshold production of mesons $\pi, 2\pi, \eta, \pi\eta, 2\eta, \rho, \omega, \ldots$
   - structure of mesons: formfactors, polarizabilities
   - mesonproduction in the region of the resonances

3. Strange Hadrons - Strangeness in Strongly Interacting Systems

- strange meson production at threshold: chiral dynamics
- K^0 formfactors
- hyperons: formfactors, polarization, resonances
- hypernuclei: momentum distribution of Λ in the nucleus,
  separated L/T structure functions

4. Parity Violation in Electron Scattering

- electric and magnetic flavour singlet form factors:
  strangeness in proton and neutron
- transverse polarization $\curvearrowright$ two photon exchange

5. Few Nucleon Systems

- structure of few nucleon systems:
  wave functions, MEC, RC, BC, ...
- GDH sum rule in few nucleon systems
- $E2/M1$ ratio for bound nucleons
- mesons in the nuclear medium

Nucleon Resonances

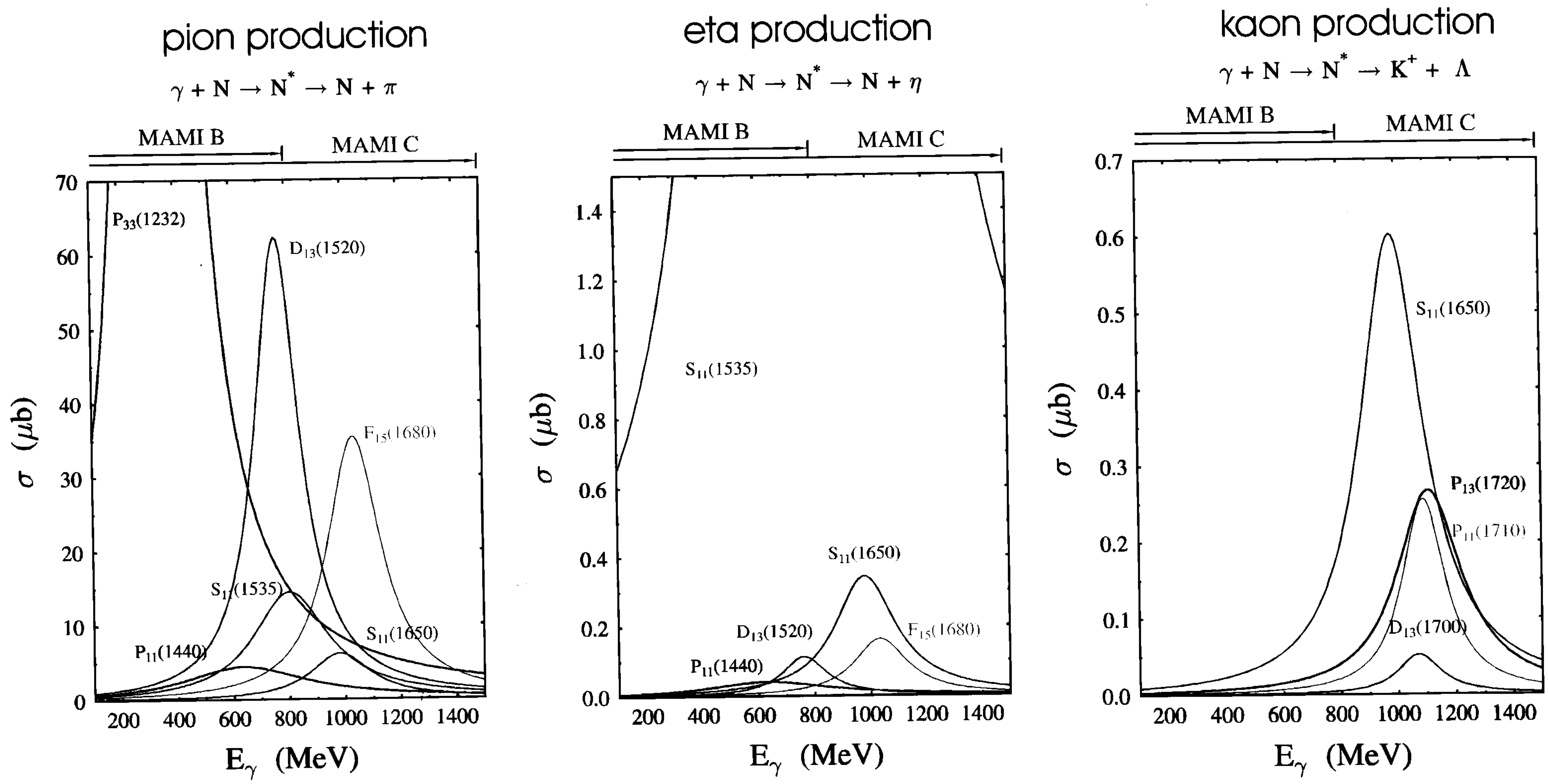

Problem : overlapping resonances

Solution : polarization observables

MAMI C : polarized photons, polarized targets and recoil-proton polarimeter

Nucleon Resonance

1951 E. Fermi : $\pi^+ + p \rightarrow p + \pi^+$ discovery of the first nucleon resonance $P_{33}(1232)$

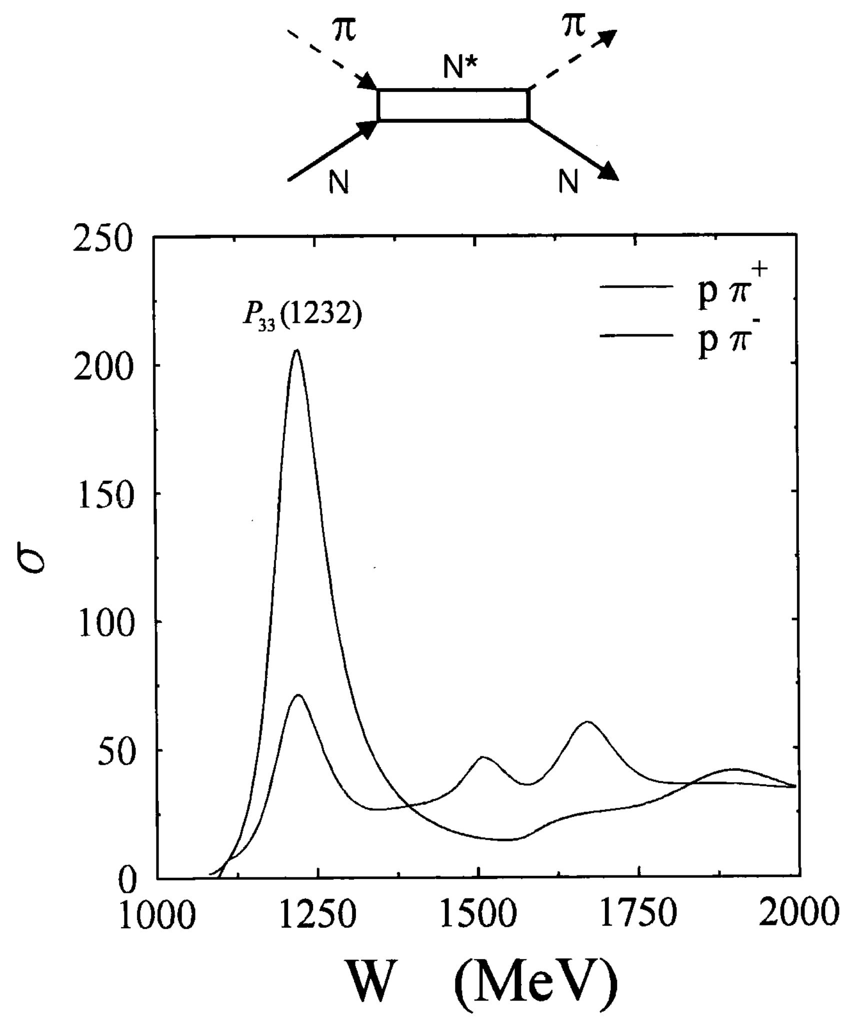

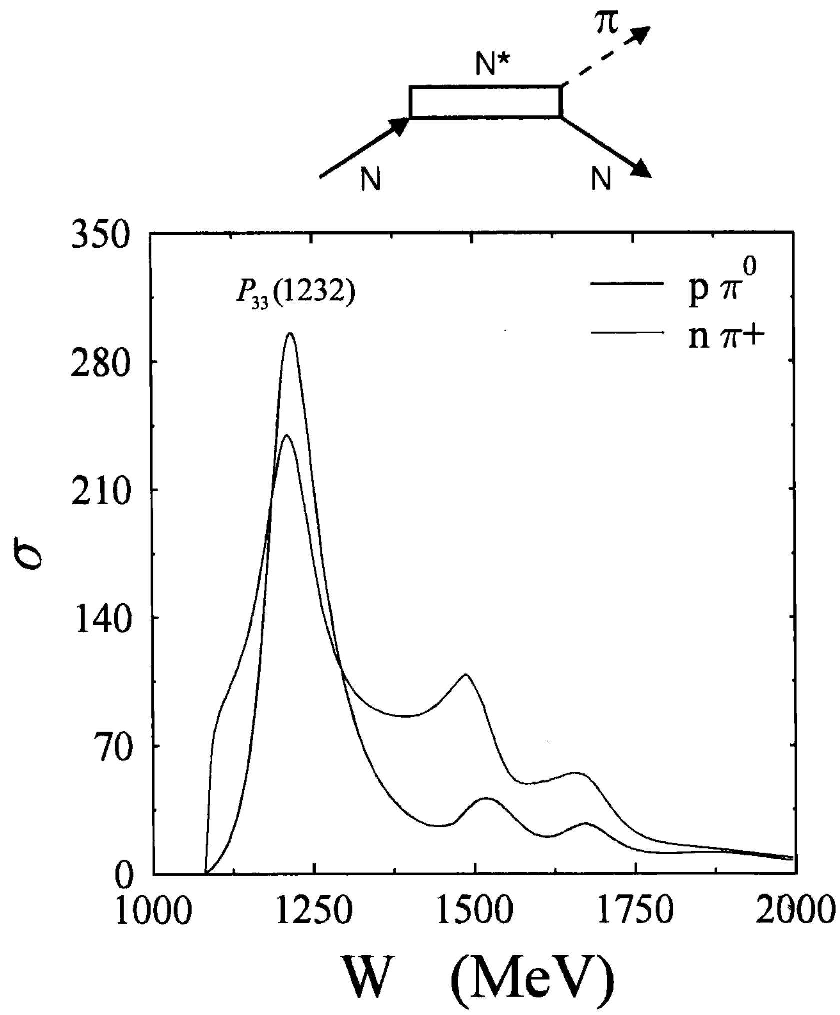

$\Delta^+(1232)$ Resonance

$\Delta^+(1232)$ resonance nucleon first excited state

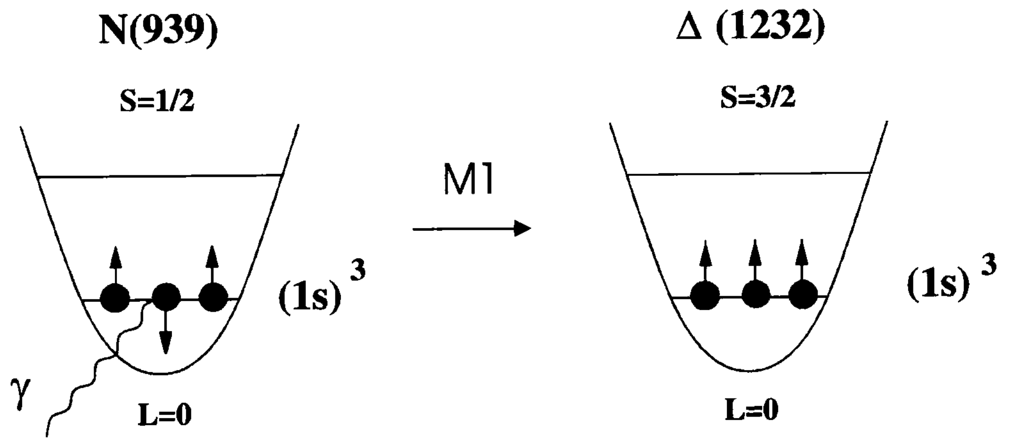

precise electro- and photoproduction data : $\gamma + p \rightarrow \Delta^+ \rightarrow \pi^0 + p$

magnetic dipole transition M1

electric quadrupole transition E2

Coulomb quadrupole transition C2

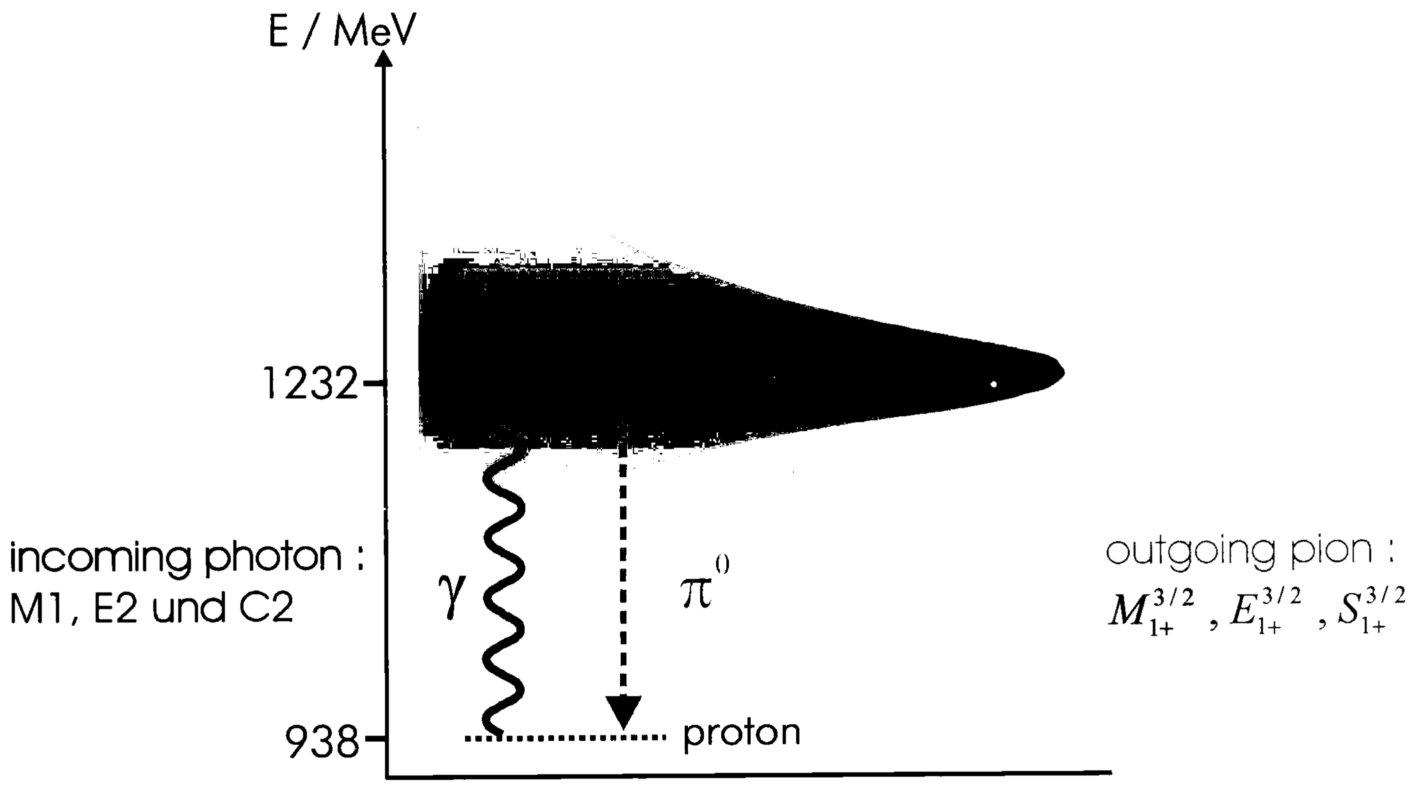

$\Delta^+(1232)$ Magnetic Moment

radiative pion photoproduction: $\gamma + p \rightarrow \Delta^+ + \gamma' \rightarrow \pi^0 + p + \gamma'$

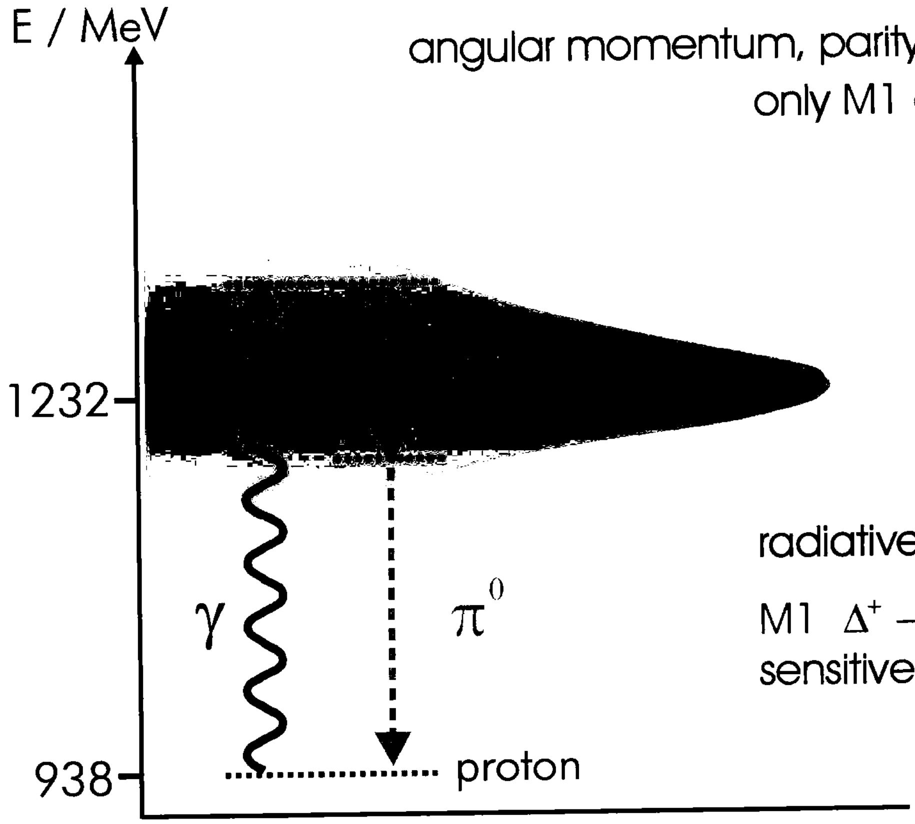

angular momentum, parity and time reversal
only M1 and M3 possible

radiative photon γ'

M1 $\Delta^+ \rightarrow \Delta^+\gamma'$ transition
sensitive to $\mu(\Delta^+)$

Δ excitation and identification
of the $p\pi^0\gamma'$ final state

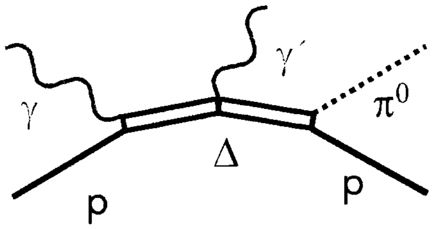

Problem :
Proton bremsstrahlung

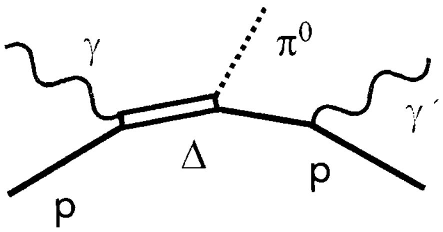

Nonresonant contributions
small in Δ-resonance region

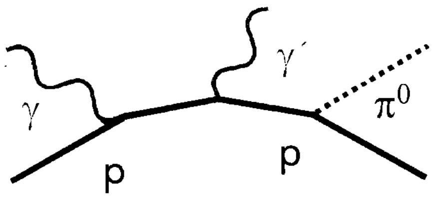

16 Polarization Observables in Meson Photoproduction

Photon		Target			Recoil			Target-Recoil			
					x'	y'	z'	x'	x'	z'	z'
		x	y	z				x	z	x	z
unpolarized	σ	0	T	0	0	P	0	$T_{x'}$	$-L_{x'}$	$T_{z'}$	$L_{z'}$
linearly polarized	$-\Sigma$	H	$(-P)$	$-G$	$O_{x'}$	$(-T)$	$O_{z'}$	$(-L_{z'})$	$(T_{z'})$	$(-L_{x'})$	$(-T_{x'})$
circularly polarized	0	F	0	$-E$	$-C_{x'}$	0	$-C_{z'}$	0	0	0	0

good experimental results only for :

σ , Σ , T , E

Observable G sensitive to $P_{11}(1440)$

$\vec{\gamma}\,\vec{p} \rightarrow p\pi^0$

Observable E sensitive to GDH sum rule

Kaon threshold production

$\vec{\gamma}\,p \rightarrow K^0\vec{\Sigma}^+$ $\quad\vec{\Sigma}^+ \rightarrow p\pi^0$ self analyzing

Roper Resonance

quark picture : $P_{11}(1440)$ radial excitation

problems :
- $M \approx 1440\, MeV \quad \Gamma \approx 350\, MeV$
- helicity amplitudes $A_{1/2}$ and $S_{1/2}$ absolute value and sign
- Q^2 dependence of $A_{1/2}$ and $S_{1/2}$

proposed solutions :
- not a |3q> excitation
- hybrid|3q g>
- $N\sigma$ molecule
- two resonances

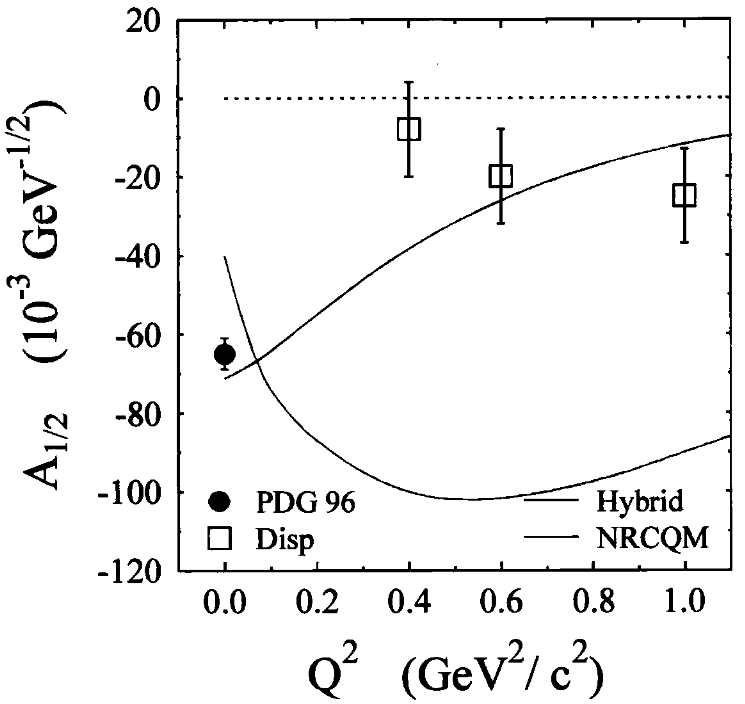

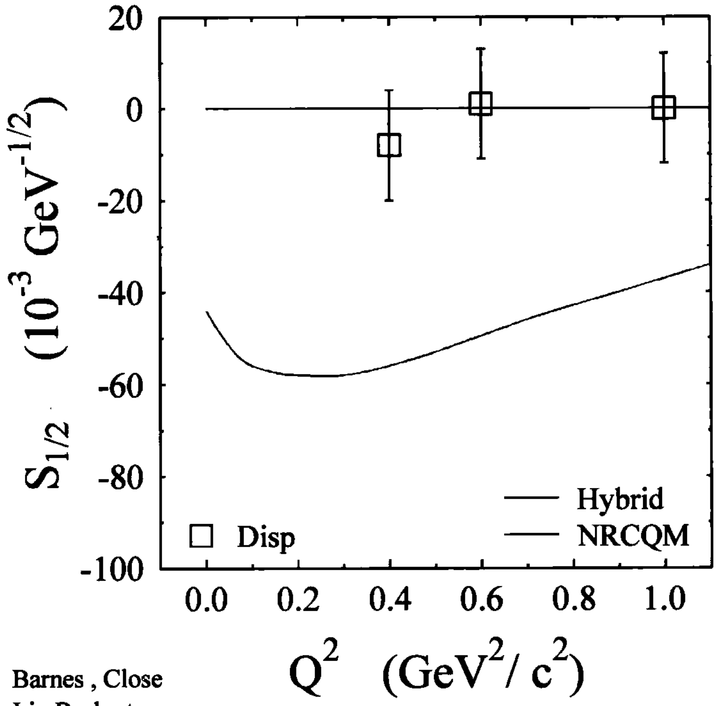

Barnes , Close
Li , Burkert

The Double Polarization Observable G

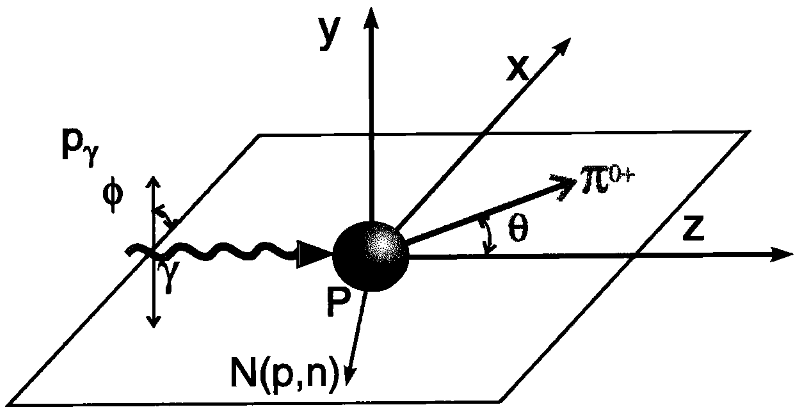

$$\vec{\gamma} + \vec{p} \rightarrow N + \pi = \left\{ \begin{matrix} n+\pi^+ \\ p+\pi^0 \end{matrix} \right.$$

$\vec{\gamma}$: linearly polarized photons

$\vec{p}$: longitudinally polarized protons

$$\frac{d\sigma}{d\Omega}(\phi, \theta) = \frac{d\sigma}{d\Omega}(\theta) \left\{ 1 - p_\gamma \Sigma \cos(2\phi) + p_\gamma p_z G \sin(2\phi) \right\}$$

$$\boxed{G \sim \mathrm{Im} M_{1-} \, \mathrm{Re} M_{1+}}$$

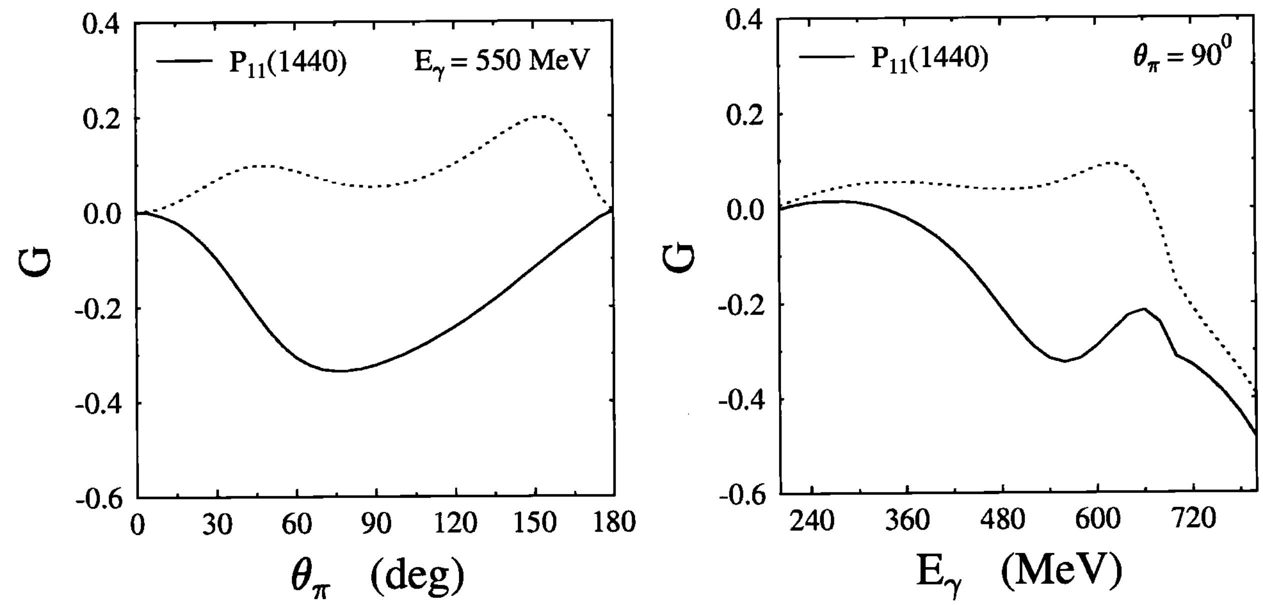

Roper Resonance

$\vec{\gamma}\,\vec{p} \rightarrow p\,\pi^0$

Asymmetry G

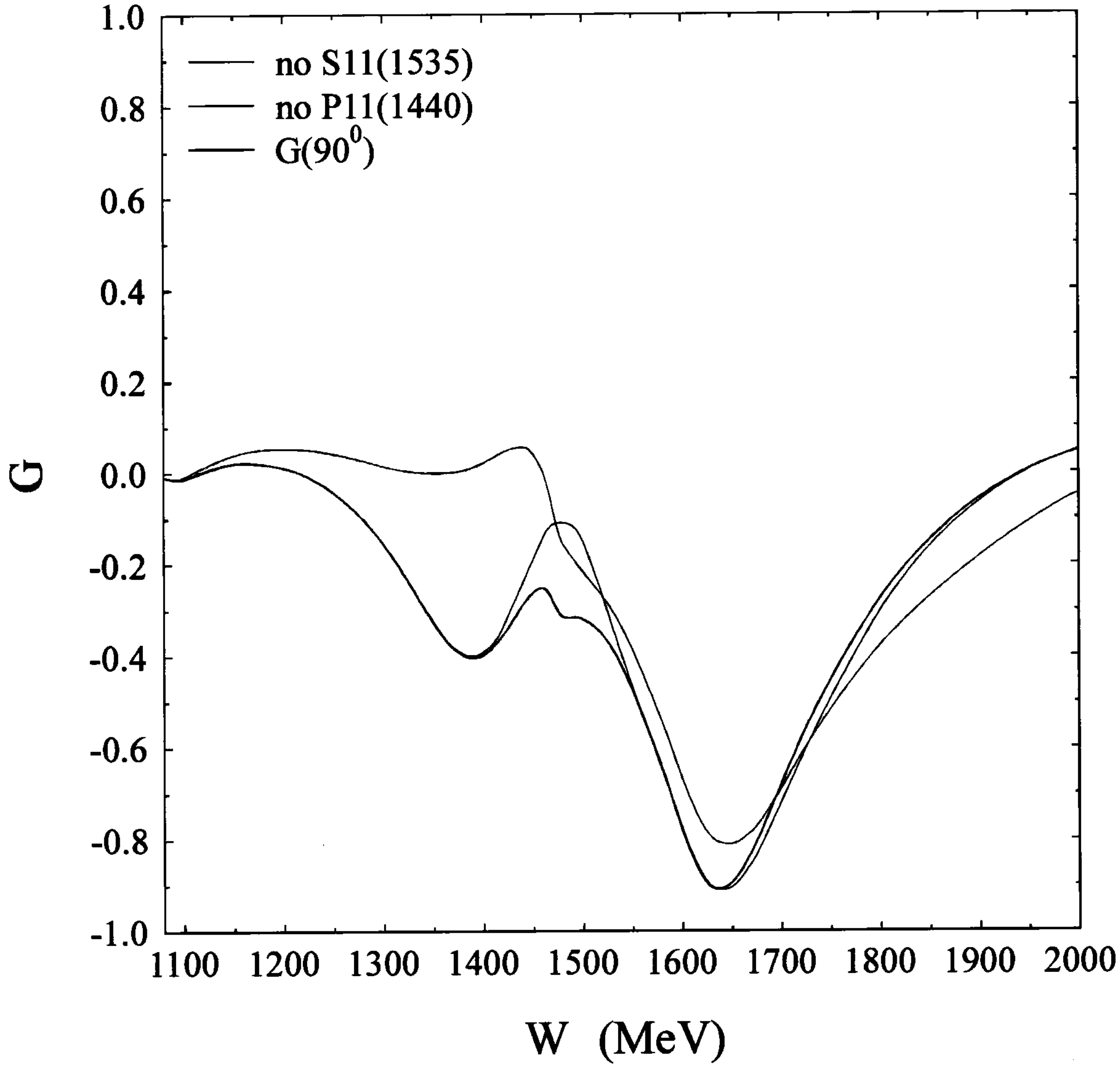

Crystal Ball @ MAMI C

SFB 443

Conclusions I

- Mainz Microtron MAMI
  produces significant information about hadrons
  - form factors of the nucleon
    2% effect at the π wavelength or larger in
    $G_{E,p}, G_{E,n}, G_{M,p}, G_{M,n}$
  - pion polarizability $(\alpha - \beta)_{\pi^+}$
    2 standard deviations from ChPTh ($\chi P\Theta$) calculations
    nature of π cloud?
  - **pion photoproduction** $p(\gamma, \pi^0)p$, $p(\vec{\gamma}, \pi^0)p$
    good agreement with ChPTh at $Q^2 = 0$
  - **pion electroproduction** $p(e, e'p)\pi^0$, $p(\vec{e}, e'p)\pi^0$
    less good agreement with ChPTh at $Q^2 > 0$
  - **helicity dependent photo production** $p(\vec{\gamma}, \{\pi^+, \pi^0, 2\pi\})$
    reasonable agreement with effective models for π^+, π^0
  - **weak form factors** $p(\vec{e}, e)p$
    first results about strangeness content of nucleon published
    experiments in broader kinematical range in progress

SFB 443

Conclusions II

- Significant hadron observables and methods
  promising connections to non perturbative QCD have emerged:
  - ∗ observable:
  - form factors and polarizabilities of baryons and mesons
  - selected resonance amplitudes below $W < 1.9\ GeV$
  - threshold reactions $(\gamma^*, \{n * \pi, K, \eta, \omega, \rho, \ldots\})$
  - ∗ experiment:
  - polarization of dense targets and high intensity beams
  - detectors with large acceptance or excellent resolution
  - ∗ theory:
  - chiral perturbation theory, QCD inspired models,
    lattice gauge theory
- MAMI B (885 MeV) 1992 - 2004
  MAMI C (1500 MeV) 2005 - 201X